Original Article

MOLECULAR METABOLISM

# Acyl CoA-binding protein in brown adipose tissue acts as a negative regulator of adaptive thermogenesis

**Albert Blasco-Roset[1,2,3], Tania Quesada-López[1,2,3,4,5], Alberto Mestres-Arenas[1,2,3], Joan Villarroya[1,2,3], Francisco J. Godoy-Nieto[1,2,3], Rubén Cereijo[1,2,3], Celia Rupérez[1,2], Ditte Neess[6], Nils J. Færgeman[6], Marta Giralt[1,2,3], Anna Planavila[1,2,3], Francesc Villarroya[1,2,3,*]**

## ABSTRACT

**Objective:** Defective activity of brown adipose tissue (BAT) is linked to obesity and cardiometabolic diseases. While much is known regarding the biological signals that trigger BAT thermogenesis, relatively little is known about the repressors that may impair BAT function in physiological and pathological settings. Acyl CoA-binding protein (ACBP; also known as diazepam binding inhibitor, DBI) has intracellular functions related to lipid metabolism and can be secreted to act as a circulating regulatory factor that affects multiple organs. Our objective was to determine the role of ACBP in BAT function.

**Methods:** Experimental models based on the targeted inactivation of the *Acbp* gene in brown adipocytes, both in vitro and in vivo, as well as brown adipocytes treated with recombinant ACBP, were developed and analyzed for transcriptomic and metabolic changes.

**Results:** ACBP expression and release in BAT are suppressed by noradrenergic cAMP-dependent signals that stimulate thermogenesis. This regulation occurs through gene expression modulation and autophagy-related processes. Mice with targeted ablation of *Acbp* in brown adipocytes exhibit enhanced BAT thermogenic activity and protection against high-fat diet-induced obesity and glucose intolerance; this is associated with BAT transcriptome changes, including upregulation of BAT thermogenesis-related genes. Treatment of brown adipocytes with exogenous ACBP suppresses oxidative activity, lipolysis, and thermogenesis-related gene expression. ACBP treatment inhibits the noradrenergic-induced phosphorylation of p38 MAP-kinase and CREB, which are major intracellular mediators of brown adipocyte thermogenesis.

**Conclusions:** The ACBP system acts as a crucial auto regulatory repressor of BAT thermogenesis that responds reciprocally to the noradrenergic induction of BAT activity.



**Keywords** Brown adipose tissue; Adipocyte; Thermogenesis; Acyl CoA-binding protein; Autophagy; Obesity

## 1. INTRODUCTION

BAT activity is known to help protect against obesity and promote cardiometabolic health in both experimental models and humans [1,2]. Traditionally, this association has been attributed to BAT's ability to oxidize metabolic fuels via the unique capacity of brown adipocytes to undergo heat-producing uncoupled mitochondrial oxidation [3] to support non-shivering thermogenesis. Within the body, BAT is a major site at which glucose and lipids are used for oxidation. Consequently, active BAT not only helps prevent obesity by increasing energy expenditure [4] it also helps prevent hyperglycemia and hyperlipidemia [5,6]. Recent work has further shown that BAT releases signaling molecules into the circulation; these so-called brown adipokines affect multiple tissues and organs dependent on the degree of thermogenic activity in BAT [7]. Although high BAT activity is generally associated with a healthy metabolic status, over-activation of BAT may be pathological in certain situations; this is seen in some cancers [8] but not in others [9] as well as in severe burn patients [10]. When BAT overactivation is pathological, it may lead to life-threatening cachectic and hypermetabolic conditions.

Extensive research has focused on determining the physiological and molecular mechanisms governing the induction of BAT thermogenesis. Studies have shown that BAT activation is mainly triggered by sympathetic signals acting on brown adipocytes [4] while some non-sympathetic signals contribute to controlling BAT activity [11]. Although it is generally assumed that impaired BAT activity can lead to metabolic and cardiovascular health problems, as seen in obesity and aging [2,12], relatively little research has explored the factors that may negatively

[1]Departament de Bioquímica i Biomedicina Molecular, Facultat de Biologia, Universitat de Barcelona, Institut de Biomedicina de la Universitat de Barcelona (IBUB), Barcelona, Spain [2]Institut de Recerca de Sant Joan de Déu, 08028 Barcelona, Spain [3]CIBER Fisiopatología de la Obesidad y Nutrición, 28029 Madrid, Spain [4]Institut d'Investigació Biomèdica Sant Pau (IIB-SANT PAU), Barcelona, Spain [5]Department of Infectious Diseases, Hospital de la Santa Creu i Sant Pau, 08041 Barcelona, Spain [6]Department of Biochemistry and Molecular Biology, University of South Denmark, DK-5230, Odense, Denmark

*Corresponding author. Departament de Bioquimica i Biomedicina Molecular, Facultat de Biologia, Universitat de Barcelona Avda Diagonal 643. 08028 Barcelona Spain. E-mail: fvillarroya@ub.edu (F. Villarroya).

Received March 13, 2025 • Revision received April 4, 2025 • Accepted April 8, 2025 • Available online 11 April 2025

https://doi.org/10.1016/j.molmet.2025.102153

 

regulate BAT activity and/or thermogenesis in response to physiological or pathological stimuli. Moreover, given the revelation that BAT impacts systemic metabolism not only via its intrinsic ability to consume fuel and sustain thermogenesis, but also through secretion of brown adipokines, it would be particularly interesting to identify the BAT-secreted molecular actors that could systemically signal low BAT activity.

Acyl CoA-binding protein (ACBP; also called diazepam binding inhibitor, DBI) is a multi-functional protein that acts both extracellularly and intracellularly to regulate multiple tissue processes including lipid metabolism and brain [13]. In skin, ACBP is required to maintain the epidermal barrier function and systemic metabolic and thermoregulatory homeostasis [14]. ACBP appears to be secreted systemically in response to autophagy activation [15]. Whole-body genetic invalidation of *Acbp* protects against obesity likely due to altered epidermal barrier that leads to increased cold sensation and energy expenditure in mice [14]. Other studies attribute obesity protection in mice with genetic invalidation of *Acbp* or antibody mediated blockage of systemic ACBP to reduced food intake and induction of anti-obesogenic metabolic pathways [15]. Recent data indicate that antibody-mediated blockage of systemic ACPB elicits pleiotropic improvements in health status acting on multiple tissues and organs [16]. However, the role of ACBP in BAT was unknown. Here, we show for the first time that the *Acbp* gene is strongly repressed by the thermogenic activation of BAT and we identify ACBP as a powerful negative regulator of BAT activity, contributing to the regulation the energy balance and metabolism.

## 2. METHODS

### 2.1. Mouse studies

C57BL/6J mice were obtained from Harlan Laboratories (Indianapolis, IN, USA). The targeted brown adipocyte-ACBP knockout (*Acbp* BAd-KO) model was generated by crossing floxed *Acbp* mice (*Acbp*$^{fl/fl}$, also used as controls) [14] and transgenic *Ucp1-Cre* mice (B6.FVB-Tg(Ucp1-cre) 1Evdr/J) obtained from Jackson Laboratory (Bar Harbor, ME, USA). Only single-copy transgenic *Ucp1-Cre* mice were used. Mice were housed at 21 °C under a 12-h light cycle (lights on from 08:00 am; lights off at 08:00 pm) with 50% ± 5% relative humidity and free access to water and a standard diet. For experiments determining the responsiveness to environmental temperatures, male mice were exposed to 30 °C for 1 week (thermoneutrality), exposed to 4 °C for 24 h or 1 week; when indicated, the mice were returned to 21 °C after the 1-week acclimation to 4 °C. When indicated, mice were treated with daily intraperitoneal (i.p.) injections of hydroxychloroquine (50 mg/kg body weight; to inhibit autophagy) or PBS (control) at the start of deacclimation and daily thereafter for 1 week, according to previously established procedures [17]. Mice were either fed a standard rodent diet (2018, Teklad Diet, Envigo, VA, USA) or, where indicated, fed a high-fat diet (HFD; #D12451, 45% Kcal fat, Envigo, VA, USA). For the HFD feeding setting, male mice were switched to HFD when 3 month-old.$VO_2$ consumption and $VCO_2$ production by individual mice were measured in Labmaster metabolic cages (TSE, Bad Homburg, Germany) after 2 days of adaptation. The surface temperature at the site of iBAT and in eye weredetermined by infrared thermography as previously described [18] using a T335 infrared digital thermal imaging camera (FLIR Systems, Wilsonville, OR, USA) and analyzed using the FLIR Quick Report 1.2 software (FLIR Systems). For tissue analysis, mice were sacrificed by decapitation and tissues were dissected and immediately snap-frozen in liquid nitrogen. Blood was also collected for plasma separation and further analysis.

### 2.2. Rat studies

Male Wistar rats (Janvier Labs, Le Genest-Saint-Isle, France) were assessed for ACBP levels in Sulzer's vein, as previously described [19]. Briefly, 8-week-old rats were exposed to 4 °C for 24 h under a 12-h light/dark cycle and feeding of a standard rodent diet (2018, Teklad Diet, Envigo). Rats were anesthetized by i.p. injection of sodium pentobarbital (50 $mg \cdot kg^{-1}$ BW). Sulzer's vein, which drains blood flowing through iBAT, was exposed. A small incision was made, a heparinized capillary was placed on the incision, and blood was allowed to flow directly into the capillary. Blood samples were centrifuged to obtain plasma, and iBAT was excised and snap-frozen in liquid nitrogen. All experiments involving mice and rats were conducted in accordance with European Community Council Directive 86/609/EEC and the National Institutes of Health guidelines for the care and use of laboratory animals. All experimental procedures were approved by the Institutional Animal Care and Use Committee of the University of Barcelona, Spain.

### 2.3. Measurements of metabolites, hormonal factors, and cytokines

Blood glucose and triglyceride levels were quantified using an Accutrend System (Roche Diagnostics GmbH, Mannheim, Germany). Plasma levels of lactate and glycerol were measured using commercially available kits (#MAK329 and #F6428, respectively; Sigma—Aldrich, St. Louis, MO, USA). Insulin and cytokines were measured in plasma samples and cell culture media using a Multiplex system (MADKMAG-HK, Merck Millipore, Rahway, NJ, USA). ACBP levels were quantified using commercially available kits applied to cell culture media from human cells cell lines (#KA0532; Abnova, Taipei, Taiwan) and mouse samples (#MBS2025156; MyBioSource, San Diego, CA, USA). For glucose tolerance tests, glucose in aqueous solution was administered i.p. (2.5 g glucose/kg) to mice that had been fasted for 6 h.

### 2.4. Separation of iBAT to brown adipocyte and stromal vascular fractions

Tissue was digested at 37 °C with type II collagenase at 15 mg per gram of tissue for 30 min in oxygenated Krebs solution (pH 7.4) containing 20 mM HEPES, 3 mM glucose, and 3.5% fatty acid-free BSA, under maximal agitation. Tissue digests were filtered, floating mature brown adipocytes were collected, and the subnatant was taken as the stromal vascular fraction (SVF) containing all non-adipocyte cells. The cell fractions were pelleted by centrifugation (20 min, 500 × *g*, 4 °C) and total RNA was extracted separately from the brown adipocyte fraction and SVF.

### 2.5. Cell culture experiments

For primary brown adipocyte differentiation, stromal vascular cells were obtained from iBAT of 3-week-old Swiss mice (Charles River, MA, USA). Differentiation of confluent precursor cells was induced using Dulbecco's modified Eagle's medium (DMEM)/F12 medium containing 10% fetal bovine serum (FBS), 20 nM insulin, 2 nM triiodothyronine (T3), and 0.1 mM ascorbic acid, according to previously established procedures [20]. Experiments were performed on day 10 of culture, when more than 90% of cells were differentiated.

Immortalized brown adipocytes from C57BL/6 J mice [21] were collected at passage 12, seeded in 6-well plates in DMEM containing 10% FBS, 20 mM HEPES, 1 nM T3, and 20 nM insulin, and grown at 37 °C in a humidified 95% air/5% $CO_2$ incubator. When cultures reached 70—80% confluence, 500 nM dexamethasone, 1 μM rosiglitazone, 125 μM indomethacin, and 500 μM 3-isobutyl-1-

 

methylxanthine were added. The cells were incubated for 2 days, changed to medium containing T3 and insulin, and incubated until they were fully differentiated (day 7).

Human SGBS pre-adipocytes at passage 10 (PCS-210—010; ATCC, VA, USA) were differentiated into mature brown/beige adipocytes using established procedures [21]. Briefly, SGBS preadipocytes were grown to confluence in DMEM/F12 medium containing 10% FBS, and differentiation was induced by incubation for 7 days in FBS-free DMEM/F12 medium containing 20 nM insulin, 0.2 nM T3, 100 nM cortisol, 25 nM dexamethasone, 500 μM 3-isobutyl-1-methyl-xanthine, and 2 μM rosiglitazone. The cells were then switched to DMEM/F12 medium plus 20 nM insulin, 0.2 nM T3, and 100 nM cortisol, and maintained for up to 14 days; during this time more than 90% of the cells acquired a fully differentiated multilocular adipocyte morphology. Where indicated, differentiated brown adipocytes and/or SGBS adipocytes were treated with 0.5 μM norepinephrine (NE; #A0937, Sigma—Aldrich), 1 mM dibutyryl-cAMP (D0627, Sigma—Aldrich), ACBP recombinant protein (#OCPD02664, Aviva Systems Biology, San Diego, CA, USA), 1.30 μg/mL anti-ACBP antibody (#ab231910, Abcam, Waltham, MA, USA), and/or 1.30 μg/mL IgG isotype antibody (#ab171870, Abcam).

For ATG7 depletion, immortalized brown pre-adipocytes were infected with a lentiviral vector encoding an shRNA against *Atg7* (si*Atg7*) or scrambled shRNA (Ctrl-siRNA), as previously described by Singh et al. (2009) [22].

### 2.6. RNA extraction and quantitative real-time PCR

Total RNA was extracted using a NucleoSpin RNA kit (Macherey—Nagel, Dueren, Germany), and 0.5 μg of total RNA was reverse transcribed using a High Capacity RNA-to-cDNA Kit (Applied Biosystems, Foster City, CA, USA). Samples were systematically checked to confirm that there was no amplification in the absence of reverse transcriptase. Quantitative real-time PCR was performed using a TaqMan system, with each reaction containing 10 μL Platinum qPCR SuperMix-UDG with ROX (Thermo Fisher Scientific), 8 μL milli-Q water, 1 μL TaqMan probe, and 1 μL cDNA. The utilized assay probes are listed in the Supplementary Table 1. cDNA levels for the gene of interest were normalized to that of the reference control (*Ppia*) using the comparative $C_T(2^{-\Delta\Delta CT})$ method. A transcript was considered non-detectable when the CT value greater than or equal to 40.

### 2.7. Mitochondrial respiration-related parameters

Oxygen consumption rate (OCR) and extracellular acidification rate (ECAR, a surrogate measure of glycolytic activity toward lactate) were determined using the Agilent Seahorse XFe24 system (Agilent, Santa Clara, CA, USA). Briefly, ∼20,000 immortalized mouse brown adipocytes/well were plated in gelatin precoated Seahorse XFe24 Cell Culture Microplates. After 24 h, the medium was switched to Agilent Seahorse XF Base Medium supplemented with 2 % BSA fatty acid-free (A8806, Sigma—Aldrich), 5 mM glucose, 0.5 mM pyruvate, and 2 mM glutamine. For determination of OCR parameters, the following were sequentially added to cells: 5 μM oligomycin (O4876), as an ATP-synthase inhibitor; 2 μM carbonyl cyanide p-(trifluoromethoxy) phenylhydrazone (FCCP; C2920) as a mitochondrial uncoupler; 5 μM rotenone (R8875), as a respiratory complex I inhibitor; and 15 μM antimycin A (A8674) (all from Sigma—Aldrich), as a respiratory complex III inhibitor. When indicated, the effects of 0.5 μM isoproterenol in the presence of 2% fatty acid-free BSA were determined, according to Li et al. [23].

### 2.8. RNAseq

Twelve week old-mice were used for RNAseq analysis of iBAT. RNA sample integrity was determined using a Qubit RNA IQ Assay (Invitrogen). Purified mRNA (2 μg) was processed using a TruSeq RNA sample prep kit v2 (Illumina). Adaptor ligation, 100 basepair (bp) cDNA fragment purification, fragment amplification, and library preparation were performed according to the manufacturer's instructions, and the generated library was sequenced using an Illumina NovaSeq 6000 platform at Centro Nacional de Análisis Genómico (Barcelona, Spain). The sequenced 100-bp paired-end reads were quality checked using FastQC and quality control alignment. The obtained reads were aligned to the mouse reference genome (GRCm39) using STAR (2.7.8a) and the numbers of exon reads for all RefSeq genes were counted using RSEM (1.3.0). Raw-count datasets for the expression of each gene and individual transcript are available at the Gene Expression Omnibus (GEO accession: GSE285403). Data for *Elmod2* and *Tbcd2* transcripts were excluded from the analysis on the basis of their presence in the B6.FVB-Tg(Ucp1-cre)1Evdr/J transgene [24]. Data analysis of the resulting count matrix was performed in R studio (4.3.1), and differentially expressed genes were identified using the DESeq application (V1.42.0). Under this R package, the log2 fold change (log2FC) was calculated, and the Wald test was used to determine significance ($P < 0.05$, Benjamini-Hochberg correction). Functional enrichment analysis was performed with ClusterProfiler (V4.10.0), gene ontology analysis was performed using GO, and functional protein association networks were determined using STRING [25].

For analysis of snRNA-seq of interscapular brown adipocytes from mice at room temperature (21 °C) and under cold exposure (8 °C, 2 days), available data at ArrayExpress, accession code E-MTAB-856219 were used and analyzed following the code deposited in GitHub (https://github.com/IRCGP-Lab/Macrophage-heterogeneity-after-MI), with minor modifications. Bioinformatics processing of the snRNA-sequencing data was performed with the R package Seurat (v.3.2.0) [26]. To exclude low quality cells in snRNA-sequencing, we filtered cells with an expressed gene count and total RNA molecules count fewer than 2% or greater than 98%. Additionally, cells in which more than 5% of reads corresponded to mitochondrial genes were removed. Data was log-normalized, and highly variable features were identified based on a variance stabilizing transformation (VST) method. All datasets (Room Temperature — RT and Cold Exposure - CE) were then integrated using the canonical correlation analysis (CCA) method, "Find Integration Anchors" and "Integrate Data" functions in Seurat. Principal components analysis (PCA) was performed on the integrated datasets. Based on the top 50 principal components (PCs), graph-based clustering was performed using the shared nearest neighbor (SNN) modularity optimization with resolution set to 1.1, and all cells were classified into 10 clusters. Clustering data was then applied followed by uniform manifold approximation and projection (UMAP) allowing the visualization of identified clusters in UMAP plots [27]. Average log e fold-change was used for comparison of *Ucp1* and *Acbp* expression levels between all the *Acbp*-expressor brown adipocytes from room temperature and cold exposure condition, and was then plotted into Violin Plot and Feature Plot using GraphPad Prism Software and FeaturePlot function split by condition in R, respectively. Wald test was used for comparision of statistical significance of the cold versus room temperature condition.

### 2.9. Western blot and multiplex analysis of phosphorylated proteins

Cells were lysed in ice-cold lysis buffer (Milliplex MAP buffer for Multiplexing, Merck Millipore) supplemented with 1 mM phenylmethylsulfonyl fluoride (PMSF). Equal amounts of protein were separated by sodium dodecyl sulfate-polyacrylamide gel electrophoresis (SDS-PAGE) on 15% gradient gels and blotted onto PVDF (polyvinylidenedifluoride) Immobilon-P membranes (Merck Millipore). The

 

membranes were probed with specific primary antibodies ACBP (1/2000 in-house [28] and 1/1000 #ab231910, Abcam), p62 (1/1000 #5114, Cell Signaling, MA, USA) UCP1 (1/10,000 #ab10983, Abcam), ATP5A + UQCRC2 (1/1000 #ab6721, Abcam) p-p38 (1/1000 #9211, Cell Signaling), total p-38 (1/1000, #9212, Cell Signaling), Atg7 (1/1000, #2631, Cell Signaling). Results were detected using an HRP-conjugated secondary goat anti-rabbit antibody (1/3000 #ab6721, Abcam) in conjunction with a chemiluminescence detection substrate (#WBKLS0500, Merck Millipore). Loading controls were established using Ponceau staining (PS). Quantification was performed using the iBright Analysis Software (Thermo Fisher Scientific) and the Multi Gauge V3.0 Software (Fujifilm, Tokyo, Japan). For multiplex analysis of total and phosphorylated proteins, cells were lysed and processed using MADKMAG-HK (Merk Millipore) according to the manufacturer instructions. Results were visualized using a Luminex system (Thermo Fisher Scientific).

### 2.10. Histological analysis

Tissues were fixed overnight in 4% paraformaldehyde, sectioned at 5-μm thick, and stained with hematoxylin and eosin (H&E) for further morphological investigation. Samples were processed by the HCB-IDIBAPS Biobank (B.0000575) within the ISCIII Biobanks platform, and with Biomodels. The lipid surface area was quantified with Image J 2.0 (NIH) using the panel Image > Adjust > Threshold, as described in Domingo et al. (2022) [29].

### 2.11. Statistical analysis

The data are expressed as means ± s.e.m. Results were analyzed by Student's *t*-test, one- or two-way analysis of variance (ANOVA) followed by Tukey's multiple-comparisons test or Dunnet's post-hoc test (for more than two groups or multiple time points, respectively), using the GraphPad 8 statistical software (GraphPad Software Inc., San Diego, CA, USA). Regression-based analysis with ANCOVA utilizing body weight as covariate was performed for energy expenditure analysis. *P*-values $<0.05$ were considered significant. *P*-value ranges and utilized statistical analyses are indicated in the figure legends. When indicated, Pearson's linear correlation analysis was performed and R and P-values are shown in the figure.

## 3. RESULTS

### 3.1. Thermogenic activation represses *Acbp* gene expression and release in BAT

We first examined *Acbp* mRNA levels in mice exposed to conditions designed to trigger cold-related thermogenic activation. As shown in Figure 1A (left), mice given short-term (1 day, acute cold, AC) or long-term (21 day, chronic cold, CC) exposures to an environmental temperature of 4 °C exhibited repression of *Acbp* gene expression in BAT, whereas re-acclimation of these cold-exposed mice to thermoneutrality (TN) was associated with rescue of *Acbp* gene expression. Reciprocally to *Acbp*, *Ucp1* gene expression was induced in response to cold and repressed after cold deacclimation, as expected. Concordant with the changes in *Acbp* gene expression, the plasma levels of ACBP were down-regulated upon cold exposure and restored by the return to thermoneutrality (Figure 1A, right). Similar results were obtained when we fed mice a high-fat diet (HFD), which is known to induce BAT activation and *Ucp1* gene expression [30]. In HFD-fed mice, *Acbp* gene expression was reduced and, additionally, the expression of *Ucp1*, the marker gene of BAT thermogenic activation, was increased (Figure 1B). To examine whether changes in *Acbp* gene expression in BAT were associated with changes in ACBP secretion, we exposed rats to an environmental temperature of 4 °C for 24 h and determined the ACBP levels in blood samples obtained from Sulzer's vein, which drains most of the blood flow from interscapular BAT (iBAT), using previously reported procedures [19]. Indeed, the ACBP levels in blood samples obtained from Sulzer's vein were negatively correlated with the *Ucp1* mRNA expression level in iBAT (used to indicate the extent of thermogenic activation in the tissue) (Figure 1C). As seen in mice, *Acbp* expression in rats was down-regulated in iBAT upon cold exposure (Figure 1D). These data confirmed that thermogenic activation of BAT decreases *Acbp* expression and ACBP secretion by BAT. Given that, in mammals, *Acbp* is widely expressed in various cell types we checked whether brown adipocytes and/or other cells within BAT exhibit down-regulation of *Acbp* expression in response to thermogenic activation. Separate analyses of brown adipocytes and the stromal vascular fraction (SVF) from BAT revealed that cold exposure repressed *Acbp* mRNA expression predominantly in brown adipocytes (Figure 1E). To confirm this, we analyzed *Acbp* expression using available snRNA-seq data from BAT adipocytes isolated from mice maintained at room temperature or exposed to cold [31]. The data revealed a significant reduction in the number of brown adipocyte nuclei with high levels of *Acbp* expression in mice exposed to cold. In contrast, the number of *Ucp1*-expressing nuclei increased, as expected, in response to cold exposure (Figure 1F).

### 3.2. Noradrenergic cAMP-mediated signaling represses *Acbp* expression and ACBP release in thermogenically activated mouse and human brown adipocytes *in vitro*

To explore the cell-autonomous regulation of *Acbp* expression and release, primary-culture mouse brown adipocytes were treated with norepinephrine (NE), which mimics the sympathetic mechanisms of thermogenic activation [32]. Our results indicated that NE treatment strongly down-regulated *Acbp* mRNA levels in brown adipocytes and reduced the release of ACBP to the cell culture medium; moreover, this inversely mirrored the induction of *Ucp1* mRNA expression, which is indicative of thermogenic activation (Figure 2A). Similar results (Figure 2B) were obtained using an immortalized cell line of murine brown adipocytes (pBAT cells) [33]. Brown adipocytes treated with cAMP, which is the main intracellular mediator of noradrenergic stimuli, also showed significant repression of *Acbp* mRNA expression and ACBP release to the medium (Figure 2C). In SGBS adipocytes, which phenotypically resemble human brown adipocytes [34], cAMP treatment strongly induced *Ucp1* mRNA expression, strongly repressed *Acbp* mRNA expression, and reduced the release of ACBP to the cell culture medium (Figure 2D). Collectively, these data indicate that noradrenergic cAMP-mediated thermogenic activation of brown adipocytes can dramatically repress *Acbp* mRNA expression and ACBP protein release.

### 3.3. Repression of autophagy contributes to decreasing *Acbp* gene expression and ACBP release by thermogenically activated BAT

Previous studies have proposed that ACBP release occurs via secretory autophagy, and is thus believed to be associated with autophagic activity [35]. Considering that thermogenic activation represses autophagy in BAT [20] we explored whether autophagy might be involved in the thermogenesis-related repression of ACBP secretion. We used brown adipocytes with invalidation of the key protein for autophagy initiation and autophagosome formation ATG7 (Supplementary Fig. 1), an established model of autophagy blockage in brown adipocytes [22] and exposed these cells to NE. Our data indicated that the NE-induced down-regulation of ACBP release was blunted in cells lacking ATG7 (Figure 3A, right). Similarly, the NE-induced down-regulation of *Acbp*

 

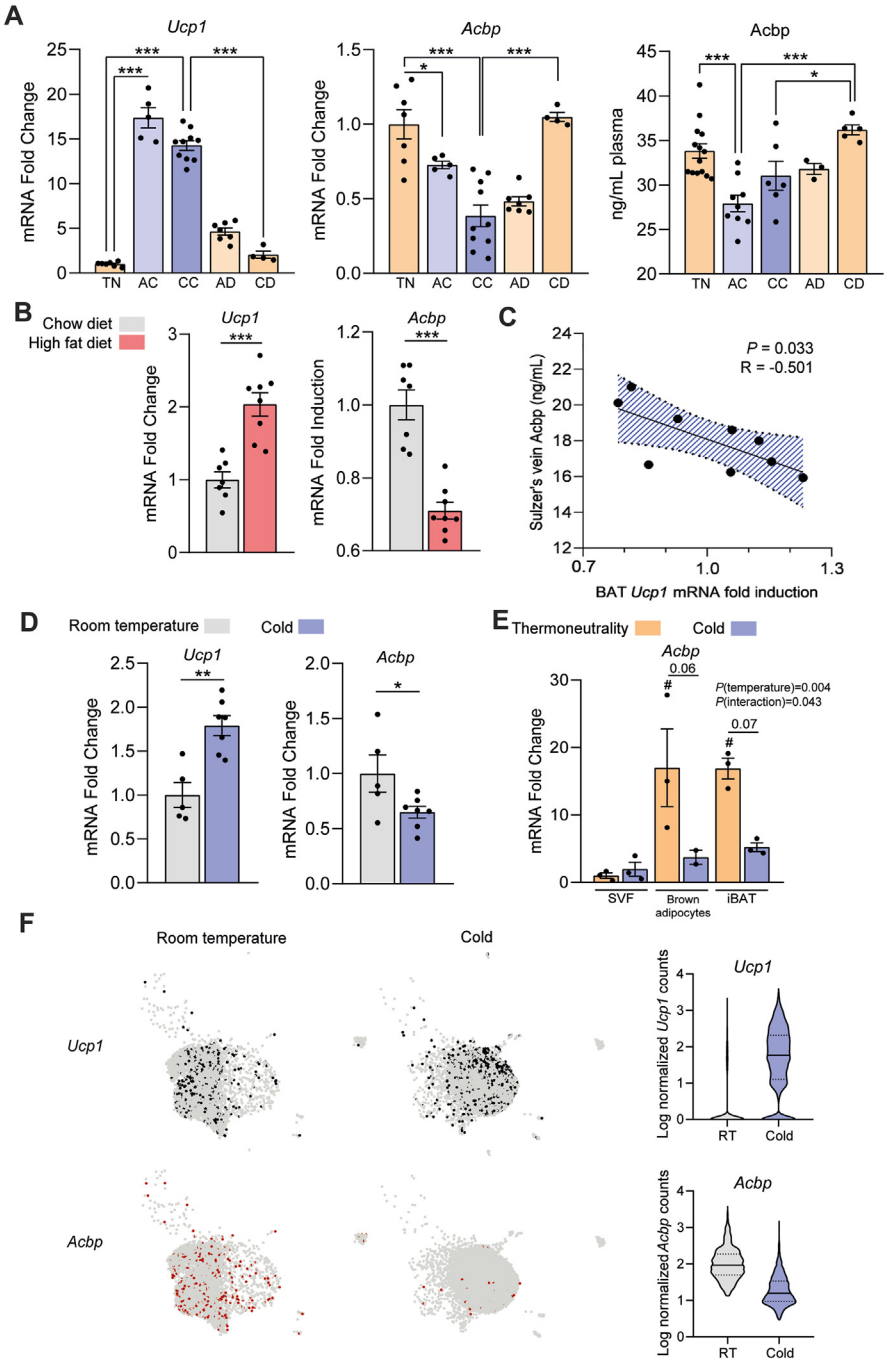


**Figure 1: ACBP expression and release are repressed by thermogenic stimuli in brown and beige adipose tissue. (A)** *Acbp* transcript expression levels in iBAT (left) and ACBP level of plasma (right) of mice exposed to cold (4 °C) for 1 day (acute cold, AC) or 21 days (chronic cold, CC), exposed to cold for 21 days and then deacclimated to thermoneutrality for 1 day (acute deacclimation, AD), or exposed to cold for 21 days and deacclimated to thermoneutrality for 7 days (chronic deacclimation, CD), as compared with transcript levels in control mice maintained at thermoneutrality (TN, 30 °C). **(B)** *Acbp* and *Ucp1* transcript expression levels in iBAT from mice fed a high-fat diet (HFD) for 12 weeks. **(C)** Pearson's linear correlation analysis of *Ucp1* transcript levels in iBAT and ACBP levels in Sulzer's vein of rats exposed to cold (24 h, 4 °C) **(D)** *Acbp* and *Ucp1* transcript expression levels in iBAT from rats exposed to cold (24 h, 4 °C). **(E)** *Acbp* transcript levels in the brown adipocyte fraction and stromal vascular fraction (SVF) from iBAT of mice exposed to cold for 24 h and controls maintained at thermoneutrality (30 °C). **(F),** Feature plots of *Acbp* and *Ucp1* expression in snRNAseq analysis of BAT adipocytes from mice at room temperature (21 °C) or exposed to cold (8 °C), left. Violin plots for *Acbp* and *Ucp1* expression, right. Expression level (y axis) refers to the log normalized ratio of gene-expression reads, normalized to the sum of all reads within each nucleus. Data in bars are means ± s.e.m. $^{*}P < 0.05$, $^{**}P < 0.01$, $^{***}P < 0.001$; as analyzed using one-way ANOVA for multiple comparisons with Tukey's post-hoc test (**A**), Pearson's correlation (*P* and R values are indicated) (**C**), or two-way ANOVA for multiple comparisons with Tukey's post-hoc test **(E)**. $^{\#}P < 0.05$ relative to SVF **(E)**. $^{*}P < 0.05$, $^{*}P < 0.01$, $^{***}P < 0.001$; as analyzed relative to controls (thermoneutrality or room temperature) using the two-tailed unpaired Student's *t*-test (**B,D).** In **(F),** $^{*}P < 0.05$ corresponds to the effects of the condition cold-versus-room temperature, according to the Wald test.

 

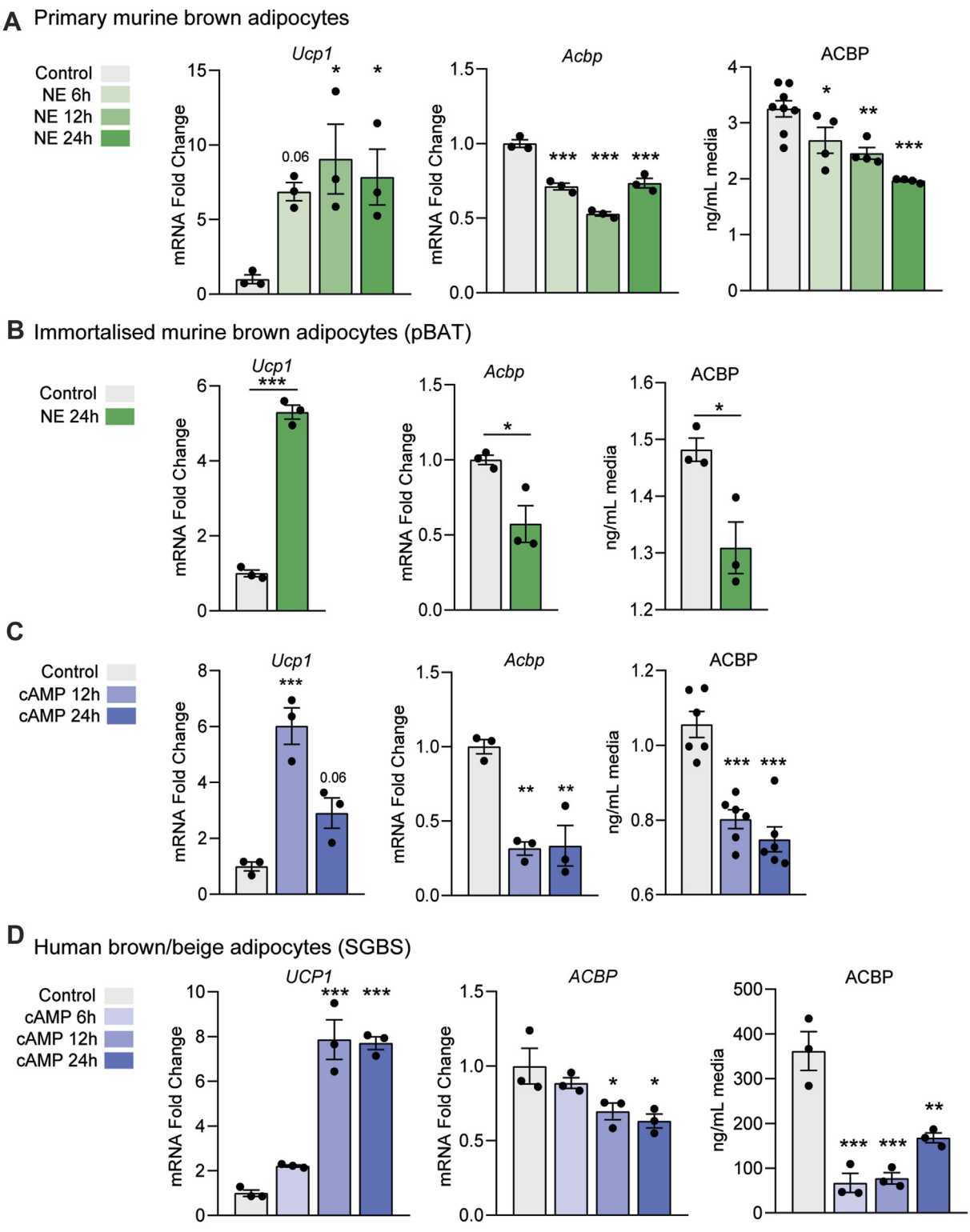


**Figure 2: Treatment with norepinephrine or cAMP represses ACBP expression and release in brown adipocytes.** *Acbp* and *Ucp1* transcript levels and ACBP protein levels in cell culture media collected from primary-culture mouse brown adipocytes (**A**), immortalized mouse brown adipocytes (**B,C**), and human SGBS brown/beige adipocytes (**D**) treated with 0.5 μM norepinephrine (NE) or 1 mM dibutyryl cAMP (cAMP), or vehicle (PBS) as control $^{*}P < 0.05$, $^{**}P < 0.01$, $^{***}P < 0.001$; as assessed relative to PBS controls using one-way ANOVA for multiple comparisons with Dunnet's post-hoc test (**A,C,D**) or two-tailed unpaired Student's *t*-test (**B**).

 

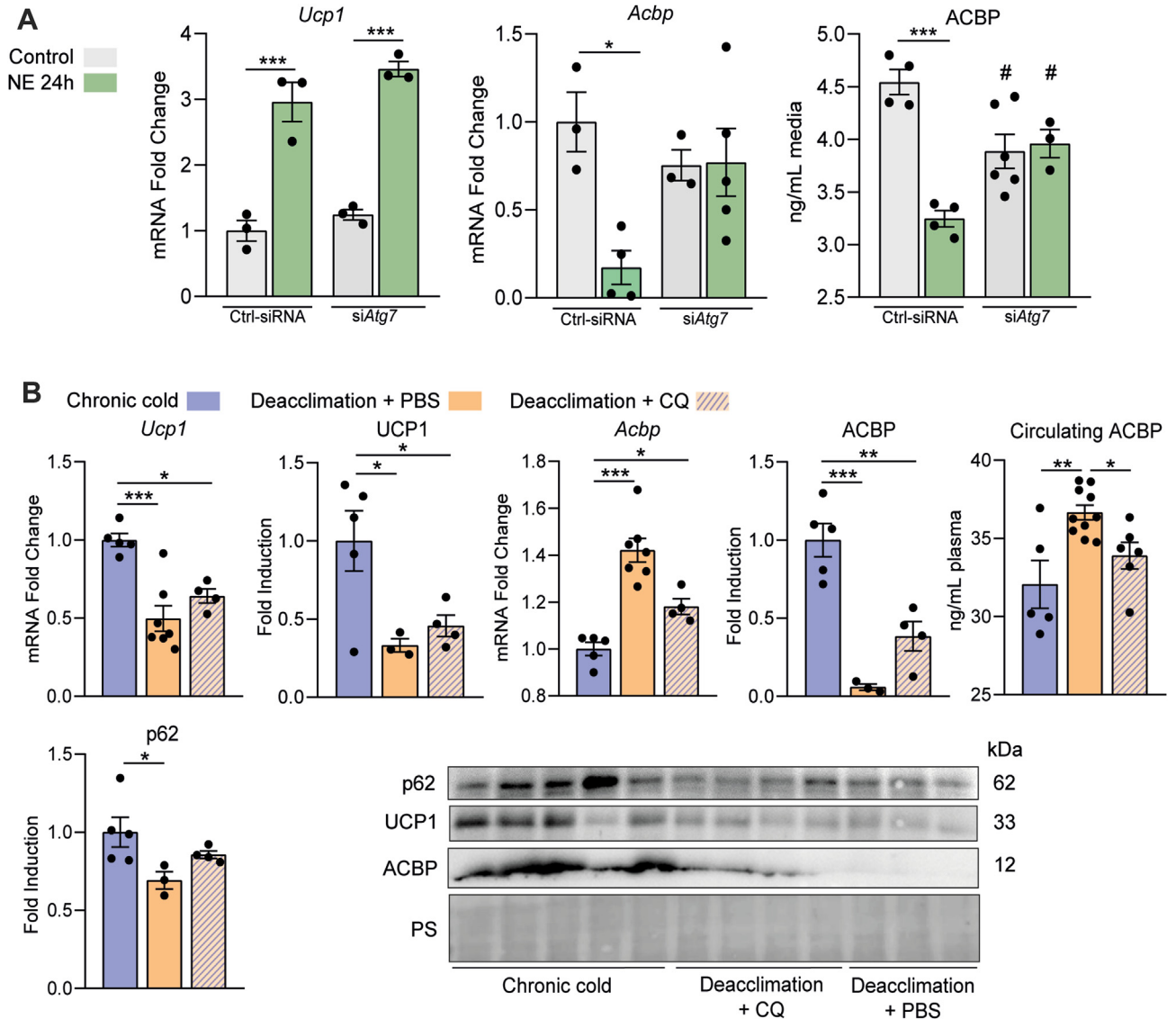


**Figure 3: Effects of autophagy inhibition on ACBP expression and release. A)** *Acbp* and *Ucp1* transcript levels and ACBP protein levels in conditioned media of mouse brown adipocytes with targeted invalidation of *Atg7* (si*Atg7*) versus control cells (scrambled siRNA, Ctrl-siRNA), under basal and 0.5 μM, 24 h norepinephrine (NE)-stimulated conditions. **B)** *Acbp* and *Ucp1* transcript levels in iBAT; UCP1, p62, and ACBP protein levels in iBAT; and ACBP protein levels in plasma, for mice exposed to cold for 10 days (chronic cold), given daily i.p. injections with 50 mg/kg chloroquine (Deacclimation + CQ) or PBS (Deacclimation + PBS). Shown is a representative immunoblot presenting results for ACBP, p62, and UCP1 and a Ponceau-stained blot. Data in bars are means ± s.e.m. (**A**) $^{*}P < 0.05$, $^{**}P < 0.01$, $^{***}P < 0.001$; as assessed by two-way ANOVA for multiple comparisons with Tukey's post-hoc test in comparisons relative to NE treatment. $^{\#}P < 0.05$ in comparisons relative to genotype (**B**) $^{*}P < 0.05$, $^{**}P < 0.01$, $^{***}P < 0.001$; as assessed by one-way ANOVA for multiple comparisons with Tukey's post-hoc test in comparisons relative to chronic cold.

mRNA expression was also suppressed in cells lacking ATG7. These data suggest that blockage of autophagy not only suppressed the post-transcriptional processes that enable secretion of ACBP, but also blunted the noradrenergic regulation of *Acbp* gene expression.

To assess whether similar changes are observed *in vivo*, we used as study model mice that were chronically exposed to cold and then returned to thermoneutrality, which results in strong up-regulation of autophagy [24] and *Acbp* expression (see Figure 1) in BAT. A group of mice was treated with chloroquine to inhibit autophagy [17]. As expected, cold-deacclimation down-regulated *Ucp1* mRNA expression and UCP1 protein levels in BAT (Figure 3B). Deacclimation caused an up-regulation of *Acbp* mRNA expression in BAT but a dramatic reduction in intracellular ACBP protein expression. This may reflect that ACBP secretion is increased due to enhanced autophagy in BAT of cold-deacclimated mice, as evidenced by reduced p62 [36] (Figure 3B, bottom). The chloroquine-induced inhibition of autophagy in cold-deacclimated mice significantly reduced the circulating levels of ACBP (Figure 3B), which is consistent with a previous report that blockade of autophagy leads to repression of ACBP secretion in tissues [15]. Our results also show that, at least in BAT, the chloroquine-induced reduction in systemic ACBP levels was associated with increased intracellular ACBP levels (likely due to accumulation caused by reduced autophagy-mediated secretion) but also reduced *Acbp* mRNA expression. Overall, these findings indicate that conditions of

 

enhanced autophagy in BAT, such as a warm environment, are associated with enhanced secretion of ACBP concomitant with increased *Acbp* gene expression.

### 3.4. Targeted ablation of *Acbp* in brown adipocytes results in thermogenic over-activation of BAT

To further explore the role of ACBP in BAT, we generated a brown adipocyte-specific *Acbp* gene invalidation mouse model (*Acbp* BAd-KO mice) by mating mice bearing *Ucp1* promoter-driven CRE with those bearing a floxed endogenous *Acbp* gene (see methods). The resulting *Acbp* BAd-KO mice showed 90% invalidation of *Acbp* transcript expression in iBAT (Figure 4A, left). Other adipose depots with a BAT-like phenotype (i.e., those with high-level expression of UCP1), such as thoracic perivascular adipose tissue (tPVAT), also showed strong invalidation of *Acbp* expression whereas the abdominal perivascular adipose tissue (aPVAT), which exhibits lower-level UCP1 expression (see Figure 5D), showed less marked invalidation of *Acbp* in our model mice (Figure 4A, left). In epididymal and inguinal white adipose tissues (WAT), the extent of invalidation was negligible. This likely reflects that, although some UCP1-expressing beige cells are present in inguinal WAT from mice, UCP1 expression is very low in mice maintained at room temperature [37]. Non-adipose tissues, such as liver, heart, and hypothalamus, did not show any invalidation of *Acbp* expression in our brown adipocyte-specific model (Figure 4A). As expected, *Acbp* BAd-KO mice showed practically undetectable levels of ACBP protein in BAT (Figure 4A). Notably, the systemic circulating ACBP levels were not affected by *Acbp* invalidation in BAT (Figure 4A, right).

Body weight was not significantly altered in *Acbp* BAd-KO mice although trended lower (Supplementary Table 2). The inguinal and epididymal WAT depots as well as iBAT were significantly smaller in *Acbp* BAd-KO mice (Figure 4B). No significant size difference was found for other tissues and organs, including the liver (Supplementary Table 2). Food intake was not significantly affected in *Acbp* BAd-KO mice (Supplementary Table 2). Glycemia and insulinemia were

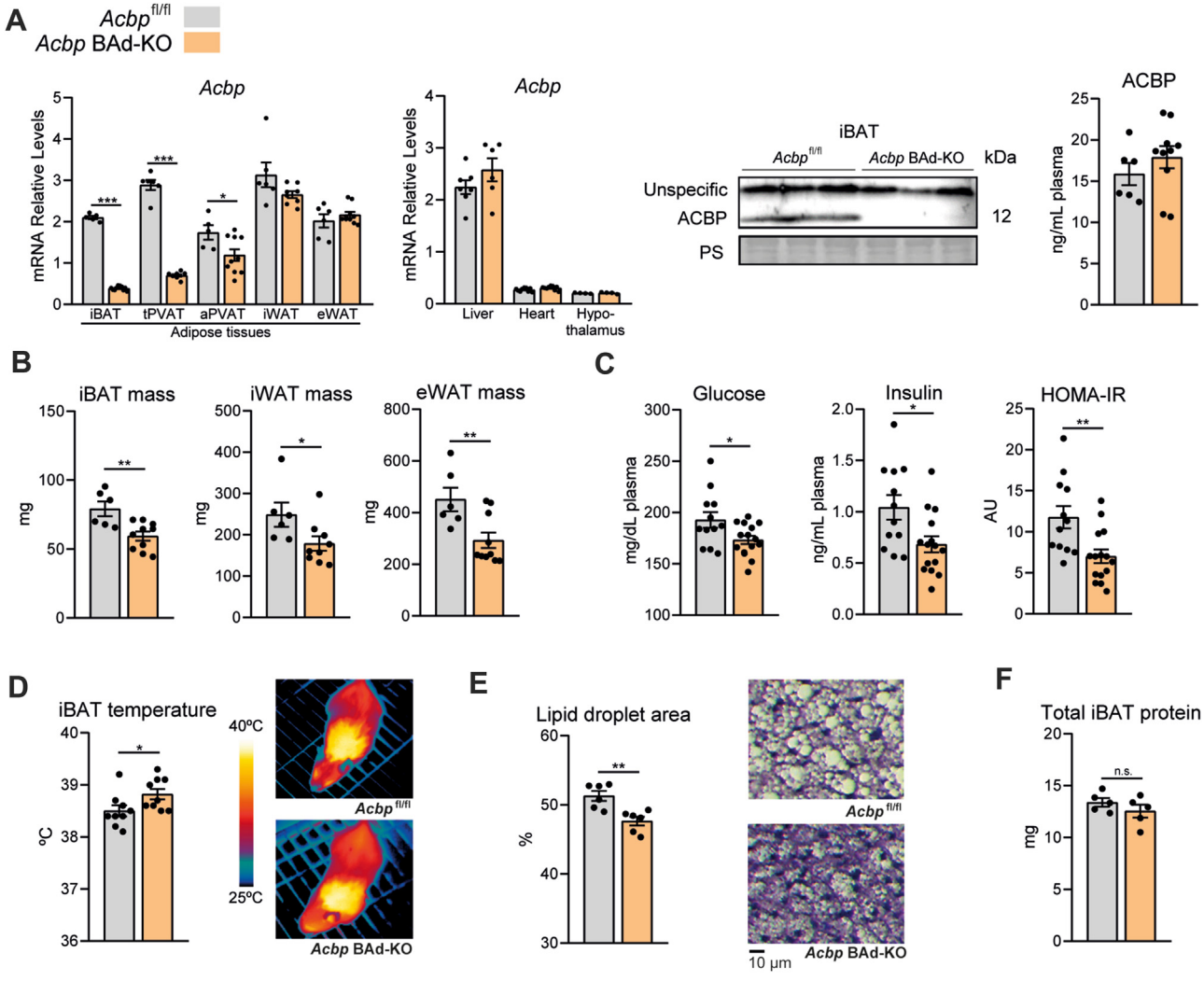


**Figure 4: Effects of brown adipocyte-specific *Acbp* invalidation in mice. A**) *Acbp* transcript levels in BAT, tPVAT (thoracic perivascular adipose tissue), aPVAT (abdominal perivascular adipose tissue), iWAT (inguinal WAT), eWAT (epididymal WAT), liver, heart, and hypothalamus of mice with targeted invalidation of *Acbp* in *Ucp1* promoter-expressing cells (*Acbp* BAd-KO). Middle, representative immunoblot of ACBP protein levels and Ponceau-stained blot. Right, plasma ACBP levels. **B)** Weights of adipose tissue depots. **C**) Plasma levels of glucose, insulin, and HOMA-IR. **D)**, Infrared-measured temperature at the iBAT region. **E**) Left, lipid droplet area in iBAT; right, representative optical microscopic images of H&E-stained iBAT. **F)** total iBAT protein content. Data in bars are means ± s.e.m. $^{*}P < 0.05$, $^{**}P < 0.01$, $^{***}P < 0.001$; as assessed by two-tailed unpaired Student's *t*-test comparing *Acbp* BAd-KO mice and *Acbp*$^{fl/fl}$ controls.

 

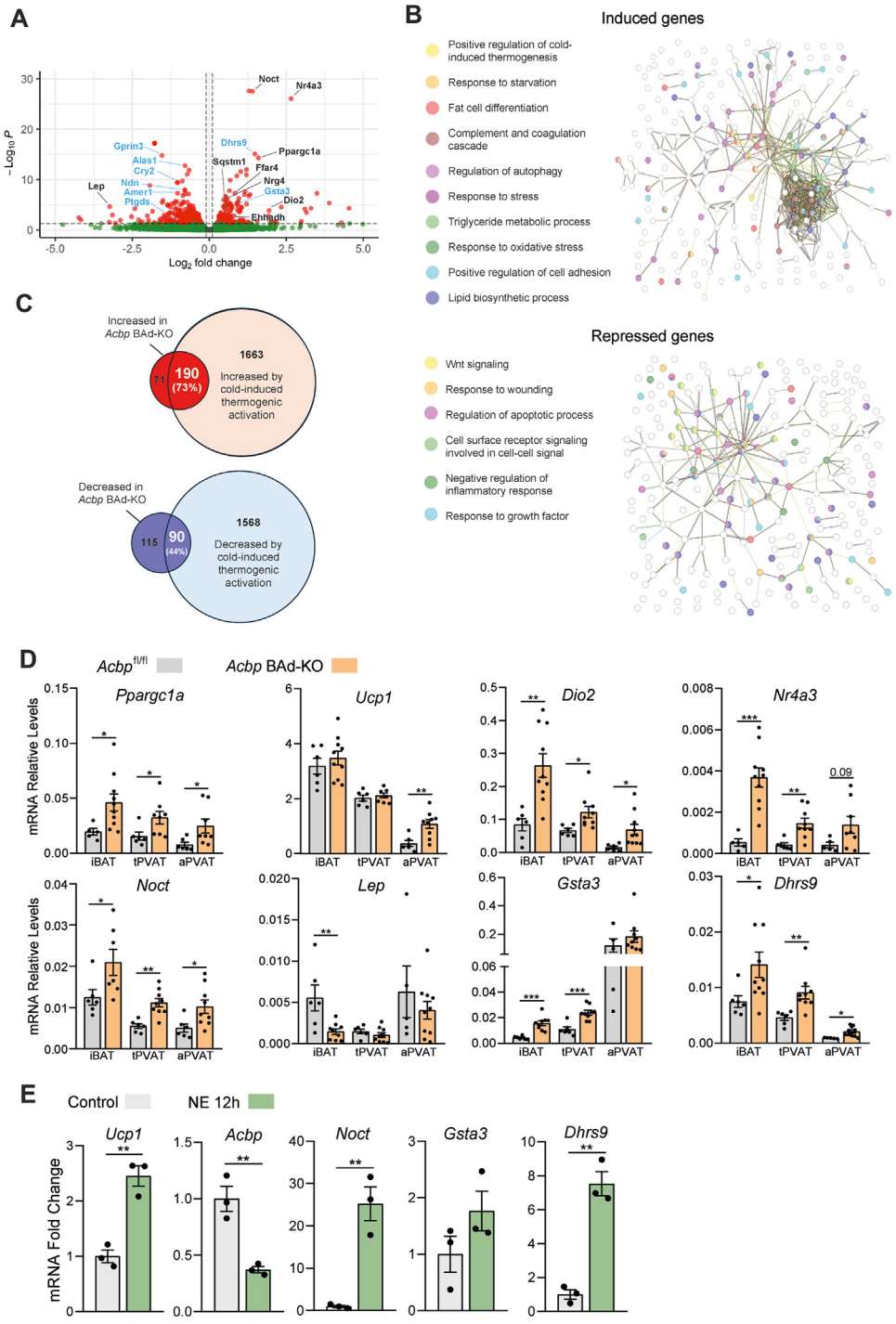


**Figure 5: Brown adipocyte-specific invalidation of *Acbp* in mice induces a thermogenesis transcriptome in iBAT.** **A)** Volcano plot depicting up-and down-regulated transcripts in iBAT from *Acbp* BAd-KO mice relative to *Acbp*$^{fl/fl}$ controls (N = 4). Statistical significance was accepted at a false discovery rate (FDR) > 1.3, adjusted *P*-value <0.05 and log2 of fold change (FC) > |0.585| (1.5-fold). Gene transcripts previously associated with BAT thermogenesis are marked in black, and those without known function in BAT are shown in blue. **B)** STRING analysis of gene transcripts up- or down-regulated in iBAT from *Acbp* BAd-KO mice relative to *Acbp*$^{fl/fl}$ controls. **C)** Venn diagram showing overlap between differentially expressed genes in iBAT from *Acbp* BAd-KO mice and those in BAT from cold-exposed wild-type mice (GSE77534). **D)** qRT-PCR analysis of the top altered gene transcripts from (**A)** in iBAT, tPVAT, and aPVAT from *Acbp* BAd-KO mice and *Acbp*$^{fl/fl}$ controls. **E)** *In vitro* effects of NE treatment of brown adipocytes on the transcript expression levels of genes up-regulated in iBAT from *Acbp* BAd-KO mice, along with those of *Ucp1* and *Acbp*. Brown adipocytes differentiated in culture were treated with 0.5 μM NE for 12 h. Data in bars are means ± s.e.m. $*P < 0.05$, $**P < 0.01$, $***P < 0.001$, as assessed by two-tailed unpaired Student's *t*-test in comparisons between *Acbp* BAd-KO mice and *Acbp*$^{fl/fl}$ controls for each adipose tissue **(D)** and for the effects of NE (**E**).

 

significantly lower in *Acbp* BAd-KO mice, thus resulting in a lower HOMA-IR (Figure 4C), indicating that the lack of ACBP in BAT improved systemic insulin sensitivity. Triglyceridemia was unaltered, as were the circulating levels of the cytokines, interleukin-6 (IL6) and chemokine (C−C motif) ligand 2 (CCL2) (Supplementary Table 2). Local infrared thermography-based assessment revealed that heat production at the iBAT region was increased in *Acbp* BAd-KO mice (Figure 4D) whereas eye temperature, a surrogate of core body temperature [18] was unaltered (not shown). Histological analysis revealed that the lipid droplets in BAT were smaller in *Acbp* BAd-KO mice, providing evidence of less fat accumulation (Figure 4E). This explained why iBAT was smaller in *Acbp* BAd-KO mice, even though the total protein content was unaltered in *Acbp* BAd-KO mice compared to control $Acbp^{fl/fl}$ mice (Figure 4F). These data are consistent with enhanced thermogenic activity in iBAT from *Acbp* BAd-KO mice.

### 3.5. Targeted ablation of *Acbp* in brown adipocytes induces an adaptive thermogenic and cold-responsive transcriptome pattern in BAT

To examine the global effects of invalidating ACBP in BAT, we used RNAseq to analyze whole-transcriptome changes of BAT from *Acbp* BAd-KO mice relative to $Acbp^{fl/fl}$ control mice. Using $P < 0.05$ as the cutoff, we identified relatively small sets of transcripts that were up-regulated (261) or down-regulated (205) in BAT under local invalidation of *Acbp* (Figure 5A,C). As expected, *Acbp* was the most highly down-regulated gene (not shown in volcano plot, for scale representation). GO-term annotation-based analysis of the up-regulated genes indicated that *Acbp* invalidation in brown adipocytes led to some induction of global pathways related to protein and lipid metabolism, including "triglyceride metabolic processes", "glycerolipid metabolic processes," and "lipid localization", as well as repression of "macroautophagy" (Supplementary Fig. 2a). GO-term annotation-based analysis of the down-regulated genes revealed inhibition of metabolic processes related to monocarboxylic acids, carbohydrates, and lipids, which is overall consistent with the ability of ACBP to function in lipid metabolism via its acyl-CoA binding properties (Supplementary Fig. 2a). STRING-based analysis of the up-regulated genes, which was used to predict alterations in protein-association networks, revealed that *Acbp* invalidation in brown adipocytes led to positive regulation of cold-induced thermogenic genes and pathways related to lipid metabolism, adipocyte differentiation, autophagy, and the complement system (Figure 5B). These findings provide evidence that, in addition to the known role of ACBP in lipid metabolism, its expression is negatively associated with BAT thermogenesis-related pathways. This is consistent with our functional results indicating that ACBP-depleted BAT exhibits increased thermogenic activity. Our STRING-based analysis of the down-regulated genes indicated that *Acbp* invalidation in brown adipocytes altered WNT signaling, which is a key pathway in adipocyte differentiation processes [38] and negatively regulated the inflammatory response, which is a crucial mediator of brown adipocyte thermogenesis [39].

The genes found to be overexpressed in BAT from *Acbp* BAd-KO mice included *Ppargc1a* (PGC1α), *Dio2*, *Nr4a3* (NOR1), *Ffar4*, *Noct*, and *Nrg4* (Figure 4A), which are known actors in BAT thermogenic activity [18,40−44]. *Ehhadh*, which is a target gene of PPARα [45], a key mediator in coupling lipid oxidation with thermogenesis in brown fat [46] was also up-regulated. Additional up-regulated transcripts, such as *Gsta3* and *Dhrs9*, corresponded to genes that have not previously been associated with BAT thermogenesis, and are not annotated as being related to thermogenesis in the GO and STRING tools. Since our STRING-based results indicated that transcripts up-regulated under *Acbp* invalidation in brown adipocytes could be related to thermogenic activation, we compared the genes significantly up-regulated in BAT from *Acbp* BAd-KO mice with the cold-responsive genes in mouse BAT, according to our previously reported transcriptomics data set [18] (GSE77534). Of the 261 gene transcripts that were significantly up-regulated in *Acbp* BAd-KO mice, 190 (73%) were significantly up-regulated in BAT in response to cold (see Figure 5C). This is particularly notable given that the cold-induced transcripts comprise only 7% of the whole transcriptome of mouse BAT [47]. Among the 205 genes down-regulated in *Acbp* BAd-KO mice, 90 (44%) were down-regulated in cold-exposed mice. Interestingly, the transcript encoding leptin, a key marker of the white-versus-brown adipose phenotype, was dramatically down-regulated (Figure 5A). However, the top-repressed genes in *Acbp* BAd-KO corresponded to genes that are either unresponsive (*Ptgds, Alas1*) or down-regulated (*Grpin3, Ndn, Cry2, Amer1*) in response to cold according to our database comparisons (GSE77534).

We validated our RNAseq data in *Acbp* BAd-KO mice by examining transcript levels in iBAT and perivascular adipose depots showing BAT-like features and significant *Acbp* invalidation (Figure 5D). Genes with known positive involvement in BAT thermogenic function, such as *Ppargc1a, Dio2*, *Noct*, and *Nr4a3*, were consistently up-regulated in iBAT, tPVAT, and aPVAT of *Acbp* BAd-KO mice. *Ucp1* expression was significantly up-regulated in the aPVAT depot. Similarly, *Gsta3*, and *Dhrs9*, which were strongly up-regulated in iBAT from *Acbp* BAd-KO mice according to our RNAseq data, were also up-regulated in the BAT-like perivascular adipose depots of these mice. In fact, the expression of *Noct* and *Dhrs9* was strongly up-regulated by NE in brown adipocytes, in a response similar to that of *Ucp1* (Figure 5E). Overall, these data support a scenario in which ACBP knockdown in BAT, in addition to altering lipid metabolism and other cellular processes, induces a transcript profile associated with BAT thermogenic activation and reciprocally down-regulates that associated with thermogenically inactive BAT. This transcriptomics-based information is consistent with the above-described functional data, and these findings together indicate that BAT is over-activated in *Acbp* BAd-KO mice.

### 3.6. Lack of ACBP at BAT protects against mice against the effects of an obesogenic high-fat diet

To assess the relevance of BAT-expressed ACBP in controlling metabolism, we analyzed the effects of an obesogenic high-fat diet (HFD) on *Acbp* BAd-KO mice. We found that mice lacking ACBP expression in BAT had significantly reduced body weight gain when given HFD during the 12 weeks of treatment (Figure 6A). That happened without significant changes in food intake ($3.11 \pm 0.11$ g/day in *Acbp* BAd-KO mice versus $3.10 \pm 0.14$ in $Acbp^{fl/fl}$ controls). In comparison with HFD-fed $Acbp^{fl/fl}$ controls, HFD-fed *Acbp* BAd-KO mice showed significantly higher energy expenditure, measured as the rate of oxygen consumption, especially during the night period (Figure 6B) which was confirmed by ANCOVA analysis using body weight as covariate (Supplementary Fig. 3). The metabolic status of *Acbp* BAd-KO mice under HFD was healthier than that of HFD-fed $Acbp^{fl/fl}$ mice, as shown by reduced basal glycemia, insulinemia, and HOMA-IR (Figure 6C), and improved glucose tolerance (Figure 6D). Histological analysis of BAT revealed that *Acbp* BAd-KO mice had a decreased lipid droplet size (Figure 6E) associated with reduced lipid content. Comparison of the BAT transcriptomes from HFD-fed *Acbp* BAd-KO mice versus HFD-treated $Acbp^{fl/fl}$ controls identified 293 up-regulated and 329 down-regulated transcripts (Figure 6F). GO annotation-based analysis of these gene sets indicated that HFD-fed *Acbp* BAd-KO mice exhibited increases in terms related to "adaptive thermogenesis", "fat cell

 

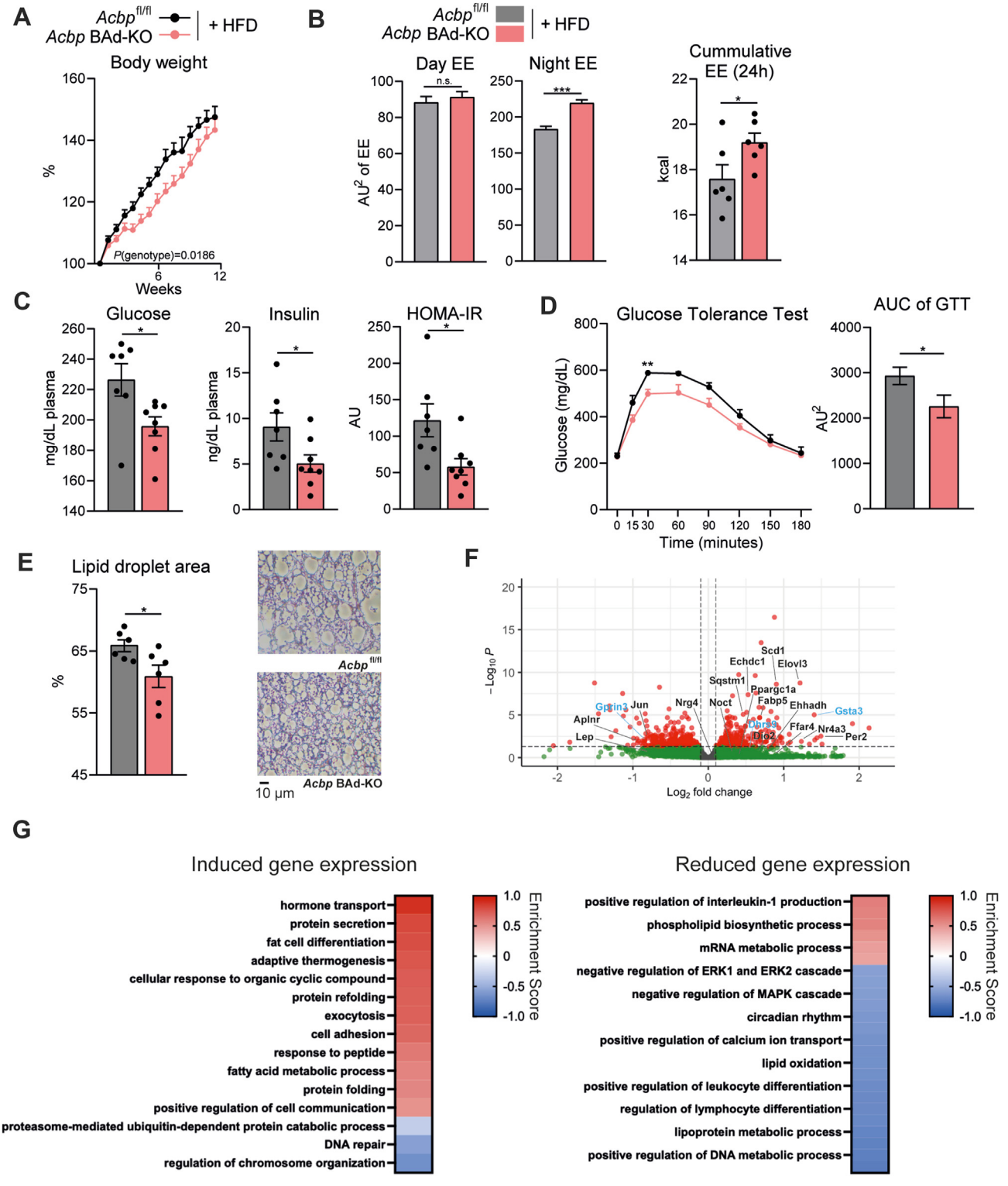


**Figure 6: Effects of HFD in mice with brown adipocyte-specific invalidation of *Acbp*.** Data show changes in *Acbp* BAd-KO mice and *Acbp*$^{fl/fl}$ controls fed HFD for 12 weeks, including changes in: **A**) body weight; **B**) daily energy expenditure, calculated as oxygen consumption; **C**) glucose and insulin levels in plasma, and HOMA-IR values; **D**) glucose tolerance curve; and **E**) lipid droplet area in iBAT (left) and representative optical microscopic images of H&E-stained iBAT (right). **F)** Volcano plot depicting overlap of up- and down-regulated transcripts in iBAT from *Acbp* BAd-KO mice relative to *Acbp*$^{fl/fl}$ controls (N = 5). Statistical significance was accepted at a false discovery rate (FDR) > 1.3 (adjusted P-value <0.05) and log2 fold change (FC) > |0.585| (1.5-fold). Gene transcripts presented in the volcano plot for standard diet-fed mice (see Figure 5) are indicated. Genes with known functions in BAT thermogenesis are marked in black, and those with unknown functions in BAT are shown in blue. **G**) Heatmap indicating the fold enrichment of GO terms (FDR/Benjamini-Hochberg ≤0.05) among genes showing up- or down-regulation in iBAT from *Acbp* BAd-KO mice relative to *Acbp*$^{fl/fl}$ controls. Data in bars are means ± s.e.m. $^{*}P < 0.05$, $^{**}P < 0.01$, $^{***}P < 0.001$; as assessed by two-tailed unpaired Student's t-test in comparisons between *Acbp* BAd-KO mice and *Acbp*$^{fl/fl}$ controls. AUC, area under the curve. AU, arbitrary units. EE, energy expenditure.

 

differentiation," "fatty acid metabolism", and some general cellular processes (Figure 6G). STRING-based analysis of the up-regulated genes identified predominant impacts on the functions of "response to heat" and "lipid metabolic processes" (Supplementary Fig. 4), whereas the corresponding analysis of down-regulated genes identified impacts on the lipid response, signaling networks involving FGFs and intracellular kinases (ERK, MAPK), the extracellular matrix, and cell adhesion (Supplementary Fig. 4). Among the main up-regulated genes in *Acbp* BAd-KO mice under standard diet feeding, the marker genes of BAT activity (*Ppargc1a, Ehhadh, Dio2, Nrg4, Nr4a3, Noct*) and *Gsta3* clustered as up-regulated genes in HFD-fed *Acbp* BAd-KO, but this induction was statistically significant only for *Nr4a3 and Gsta3*.

### 3.7. ACBP represses mitochondrial oxidation, lipolysis, and thermogenic gene expression whereas it induces inflammatory cytokine expression and secretion in brown adipocytes

Once established that *Acbp* expression in BAT is reciprocally associated with thermogenic activity in BAT, we addressed whether extracellular ACBP may contribute to regulating brown adipocyte activity. For this purpose, we treated mouse brown adipocytes with recombinant ACBP for 24 h. Our data indicated that extracellular ACBP significantly reduced oxidative parameters (basal and maximal respiration) and proton leakage in brown adipocytes (Figure 7A). This was accompanied by a reduction in extracellular acidification (ECAR), which is a surrogate for glycolytic activity. These results indicate that ACBP-treated brown adipocytes exhibit an overall impairment in metabolic activity. Moreover, we found that ACBP repressed significantly isoproterenol-induced oxygen consumption (Figure 7B), an indicator of thermogenic uncoupled respiration [23].

When we assessed components of mitochondrial oxidative (OXPHOS) and thermogenic activities, we found that brown adipocytes treated with ACBP exhibited significant reductions in the levels of ATP5A (a component of ATP synthase in OXPHOS complex V) and UCP1 (the key mitochondrial protein for thermogenesis), but not UQCRC2 (a component of OXPHOS complex III) (Figure 7C). This was associated with reduced transcript levels for *Atp5g3* (a component of OXPHOS complex V) and *Uqcrc1* (a component of OXPHOS complex III) (Figure 7D).

We then examined transcript levels for genes that mark brown adipocyte thermogenic activity and are sensitive to thermogenic stimuli, including those found to be up-regulated in BAT from *Acbp* BAd-KO mice. We observed that ACBP treatment of brown adipocytes led to the following: down-regulation of the marker genes of BAT activation *Ucp1, Ppargc1*, *Bmp8b*, and *Ehhadh* (Figure 8A); no alteration of some the cold-sensitive gene transcripts up-regulated in BAT from *Acbp* BAd-KO mice, namely *Gsta3,* and *Dhrs9*; and up-regulation of *Il6* (Figure 8B). Regarding protein secretion, we found that ACBP increased the releases of IL-6 and CCL2 (Figure 8C), ACBP also caused a significant decrease in the release of glycerol by brown adipocytes, indicating impaired lipolysis (Figure 8D).

We also determined whether extracellular ACBP affected the NE-mediated induction of thermogenic genes. Indeed, we found that treatment of brown adipocytes with ACBP decreased the ability of NE to up-regulate *Ucp1, Noct,* and *Dhrs9* (Figure 8E).

Given the above findings obtained upon 24 h treatment of differentiated brown adipocytes with ACBP, we further examined the impact of adding ACBP to the cell culture medium during the whole differentiation process, from the preadipocyte (day 1 of culture) to differentiated (day 8) stages. This treatment did not modify the differentiation of brown adipocytes, as assessed by monitoring the acquisition of brown adipocyte cell morphology (Supplementary Fig. 5a). However, similarly to the effects of ACBP in differentiated brown adipocytes, the presence of ACBP in the culture medium during differentiation was associated with down-regulation of *Ucp1, Ppargc1a* and *Bmp8b* and up-regulation of *Il6* (Supplementary Figs. 5b and c).

### 3.8. Blockage of endogenous ACBP secreted to the brown adipocyte culture medium promotes thermogenic gene expression

To assess whether the above-described effects could be directly related to the ACBP secreted by brown adipocytes, we blocked the endogenously secreted ACBP by adding a specific antibody to the brown adipocyte culture medium. Our results indicated that neutralization of endogenous secreted ACBP significantly increased the transcript levels of *Ucp1* and several genes that are involved in thermogenic activation of BAT and were found to be up-regulated in *Acbp* BAd-KO mice, including *Nr4a3 and Ehhadh* (Supplementary Fig. 6a). This blockade also decreased the expression of *Ccl2* (Supplementary Fig. 6b), although it did not result in altered secretion (Supplementary Fig. 6c). Glycerol release was dramatically induced by neutralization of ACBP in the medium, indicating enhanced lipolysis (Supplementary Fig. 6d). Overall, these results indicate that blockage of endogenously secreted ACBP induces several parameters indicative of increased thermogenic activity, partially mirroring the results found in brown adipocytes exposed to high levels of recombinant ACBP in the cell culture medium.

### 3.9. Effects of ACBP on intracellular pathways that control brown adipocyte activity

We also determined how extracellular ACBP affected phosphorylation-dependent intracellular signaling pathways of brown adipocytes in response to the thermogenic activators, NE and cAMP. Our results indicated that ACBP treatment significantly repressed the capacities of NE and cAMP to activate p38 MAP-kinase (Figure 8F), which is a major intracellular pathway known to mediate thermogenic activation [48]. The other tested intracellular mediators did not exhibit any alteration of phosphorylation status under ACBP treatment, except for the p-Akt/Akt ratio, which showed a decreasing tendency (Supplementary Fig. 7). Among the other tested intracellular regulators, the NE-induced phosphorylation of CREB, which is a key transcription factor in the noradrenergic regulation of thermogenic gene expression [49], was found to be down-regulated by ACBP (Supplementary Fig. 7). These data show that extracellular ACBP interferes strongly with key intracellular pathways that contribute to the induction of thermogenesis, mainly the p38 MAP kinase pathway.

## 4. DISCUSSION

In the present study, we show that the expression and release of ACBP in brown adipocytes is strongly inhibited by thermogenic noradrenergic-mediated stimuli, and that ACBP contributes to controlling BAT activity by inhibiting its thermogenic function.

We found that BAT activation is associated with strong repression of *Acbp* gene expression associated within reduced secretion and release of ACBP by brown adipocytes. The ability of thermogenically active BAT to impair autophagy appears to contribute to the reduced secretion of ACBP, as do noradrenergic mechanisms that transcriptionally repress *Acbp*. In fact, accumulation of intracellular ACBP protein in BAT in response to cold [50] and reduction after deacclimation (see Results) are likely to be due the reciprocal effect of cold on autophagy and subsequent autophagy-associated release of ACBP.

Targeted invalidation of *Acbp* in brown adipocytes resulted in BAT transcriptome remodeling and histological alterations consistent with enhanced thermogenic activity, which was also evidenced by

 

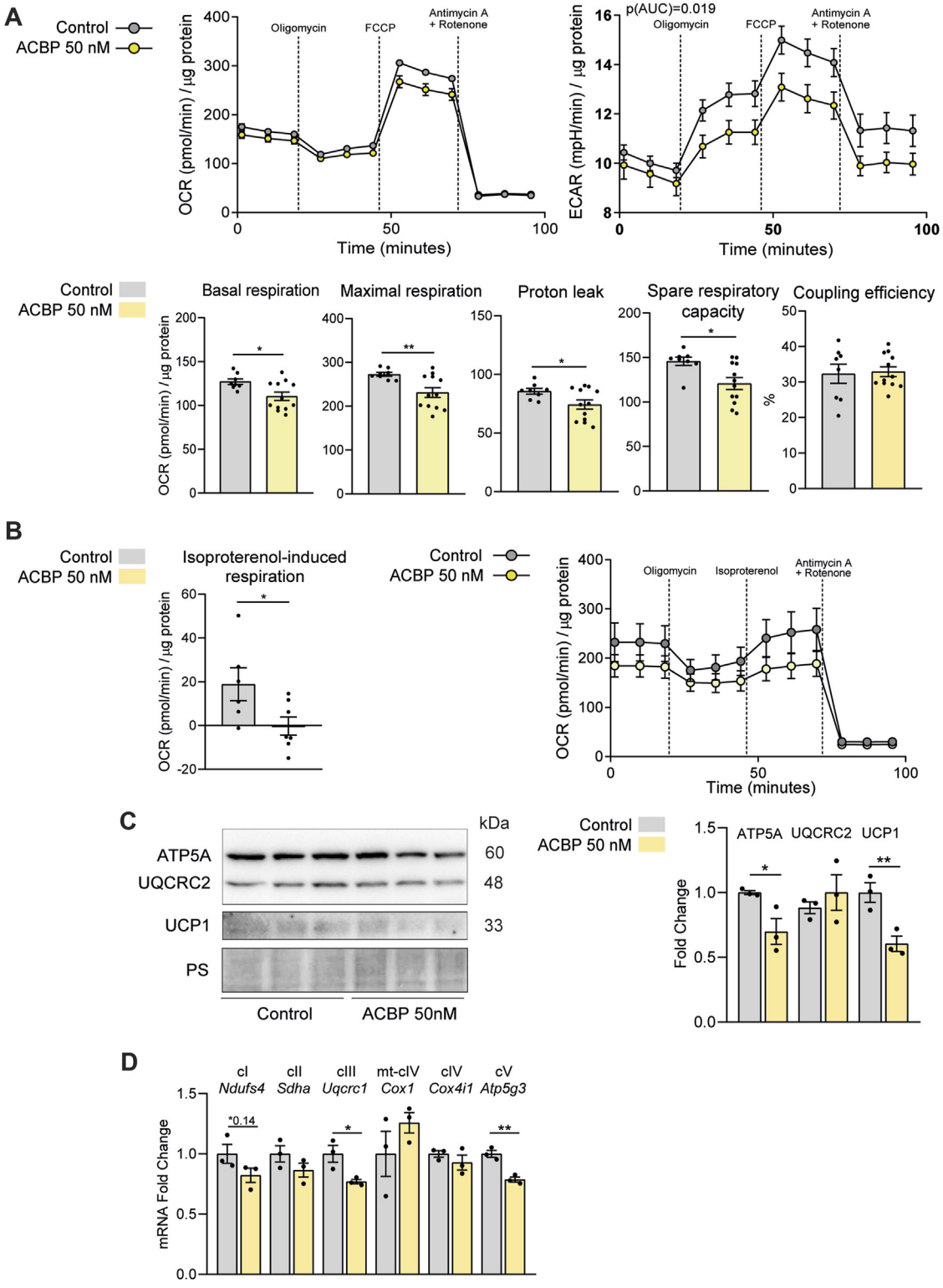


**Figure 7: ACBP reduces oxidative activity in brown adipocytes.** Mouse brown adipocytes were treated with recombinant mouse ACBP protein for 24 h. Shown are: **A)** representative profiles of oxygen consumption (OCR) and extracellular acidification (ECAR) rates (top), and respiratory parameters (bottom); **B)** oxygen consumption in response to isoproterenol (left) and representative profile (right); **C)** changes in mitochondrial OXPHOS proteins (UQCRC2 and ATP5A) and UCP1 (immunoblot, left; densitometric quantification of changes, right); and **D)** transcript levels of components of the mitochondrial respiratory chain/OXPHOS system (cI to cV, mitochondrial complex I to V). Data in bars are means ± s.e.m. $*P < 0.05$, $**P < 0.01$, $***P < 0.001$; as assessed by in two-tailed unpaired Student's *t*-test in comparisons between ACBP-treated cells and untreated controls.

 

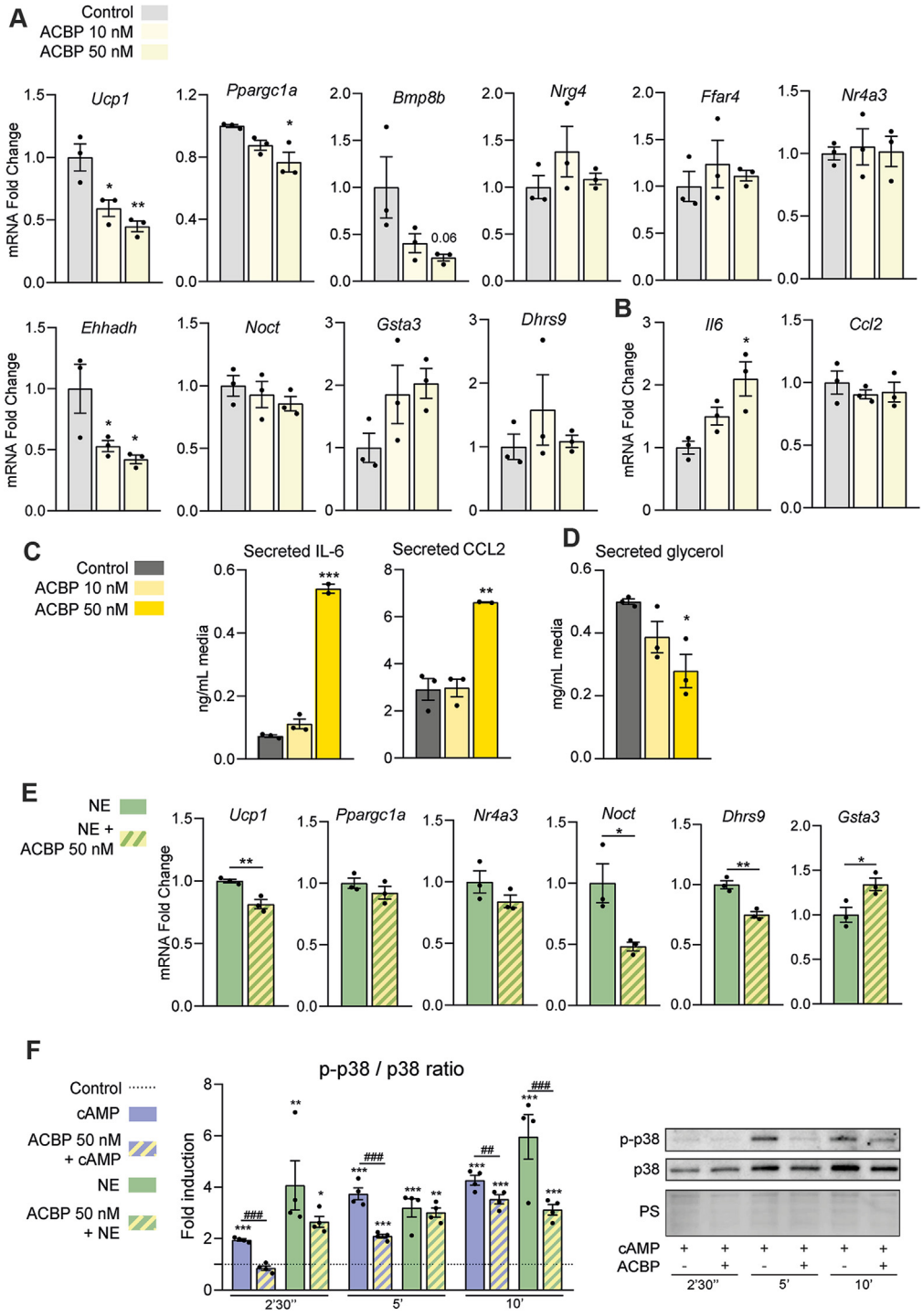


**Figure 8: Effects of extracellular ACBP on gene expression, secretory properties of brown adipocytes and regulatory intracellular kinases. A**–**C**, Mouse brown adipocytes were treated with recombinant mouse ACBP protein for 24 h. Shown are: **A**, transcript levels of thermogenic activity marker genes and up-regulated genes in iBAT from *Acbp*-invalidated mice (see Figure 5); **B**, transcript levels of the pro-inflammatory cytokines, *Il6* and *Ccl2*; **C**, levels of IL6 and CCL2 in cell culture medium; and **D**, levels of glycerol in cell culture medium. **E**, Levels of the indicated transcripts in brown adipocytes treated with ACBP alone or with 0.5 μM NE for 24 h. **F**, phosphorylated (p)-p38/P38 ratio in brown adipocytes treated with recombinant ACBP for 24 h and then treated with 1 mM cAMP or 0.5 μM NE for the indicated times (left), and representative immunoblot of p-p38 and P38 in brown adipocytes treated with ACBP and cAMP (right). Data in bars are means ± s.e.m. $^{*}P < 0.05$, $^{**}P < 0.01$, $^{***}P < 0.001$; as assessed by one-way ANOVA followed by Dunnet's post-hoc test compared to controls (**A**–**D**), two-tailed unpaired Student's *t*-test in comparisons between ACBP-treated cells and untreated controls **(E)** and two-way ANOVA for multiple comparisons with Tukey's post-hoc test, relative to untreated cells at minute 0 (dotted line) **(F).** $^{\#\#}P < 0.01$, $^{\#\#\#}P < 0.0001$; analyzed as described above, relative to ACBP-treated brown adipocytes at the same time point.

 

increased local heat production at the iBAT region. This was associated with an improved systemic metabolic status under both basal and obesogenic conditions, especially in relation to glucose homeostasis, and even protection against obesogenesis in the absence of altered food intake and in association with enhanced energy expenditure. These findings in mice with BAT-specific invalidation of *Acbp* are compatible with previous data showing that constitutive invalidation of *Acbp* expression in all adipose tissues (WAT and BAT) protects against obesity in mice [51] and highlights the importance of BAT as a site where ACBP expression affects whole-body homeostasis and metabolism. It should be noted that, as expected, the UCP1 promoter-directed invalidation of *Acbp* affected BAT-like adipose depots other than iBAT, such as perivascular adipose tissues. This indicates that changes in ACBP expression and release in these adipose depots may have systemic consequences via a local action of secreted ACBP at the vascular level occurring either directly (local effects of decreased ACBP secretion by brown adipocytes), or indirectly (overactivation of BAT due to the lack of ACBP in these anatomical locations).

Interestingly, our analysis of the BAT transcriptome in mice with *Acbp* gene invalidation identified, in addition to well-characterized marker genes of thermogenesis (e.g. *Ppargc1a*, *Dio2* …), up-regulation of transcripts that show strong inducibility in BAT when stimulated by cold and in brown adipocytes in response to noradrenergic stimulus. Among them, *Gsta3* ($\alpha$-class glutathione S-transferase) and *Dhrs9* (dehydrogenase/reductase SDR family member 9), have not been previously related to brown adipose tissue biology. Further research will be needed to ascertain the role of these novel actors in BAT activity and in relation to ACBP functions.

The effects of *Acbp* invalidation in BAT were not associated with any alteration in the circulating levels of ACBP, which may reflect that BAT contributes relatively little to systemic ACBP, and/or it may indicate that there is homeostatic compensation via increased secretion by other tissues. In any case, these findings suggest that the systemic impact of ACBP invalidation in BAT occurs through the local actions of ACBP in the tissue, which may involve intracellular and autocrine effects.

Our *in vitro* studies suggest that extracellular ACBP can strongly repress brown adipocyte thermogenic and metabolic activity and induce pro-inflammatory signaling, and that neutralization of brown adipocyte-secreted ACBP elicits some of these effects. In fact, extracellular ACBP represses the capacity of noradrenergic signals to activate intracellular p38 MAP kinase signaling and CREB phosphorylation, which are known to elicit transcriptional activation of the thermogenic program in brown adipocytes [48,49]. Although the cellular receptor responsible for mediating the action of ACBP is not fully known, published reports indicate that GABA-A receptor mediates ACBP action in the brain [13] and, more recently, that GABA-A receptor subunit gamma-2 is also involved in mediating the effects of ACBP in peripheral tissues [52]. According to our previously reported RNAseq database (GSE77534), the transcript expression levels of *Gabra2* receptors subunits are high in BAT, and the genes encoding GABA-A recepto subunits are generally down-regulated under cold-induced BAT activation (Supplementary Fig. 8). This supports the notion that ACBP/GABA-A receptor signaling may contribute to BAT thermogenic regulation. Further research is warranted to address this possibility. Moreover, consistent with previous results obtained using antibody-mediated systemic neutralization of ACBP [53] antibody-mediated blockage of ACBP in the brown adipocyte culture medium mirrors some of the effects of exogenous ACBP treatment, especially the inhibition lipolysis induction.

In summary, we herein show that the thermogenic activation of BAT suppresses ACBP expression and release, while ACBP itself strongly inhibits BAT activity, creating a self-inhibitory loop in regulating BAT function. Reciprocally, warm conditions lead to increased *Acbp* gene expression and ACBP secretion in BAT due to enhanced *Acbp* transcription and autophagy-mediated ACBP secretion, which contribute to repressed thermogenic activity. While much is known about adrenergic and non-adrenergic activators of BAT, we know less about the relevant repressors. Some, such as kininogen and sLR11 [54,55] function as local autocrine factors. These factors are paradoxically induced by noradrenergic stimuli and seem to provide rheostatic regulation of BAT to prevent excessive energy dissipation. We identify ACBP as the first BAT-secreted protein that acts as a repressor in a unique way: it directly inhibits BAT activity and shows reduced expression and release under noradrenergic stimulation. This process mediates the reciprocal coupling of thermogenic activation and ACBP-mediated repression of BAT activity. High ACBP levels are associated with obesity, diabetes, inflammation, cardiometabolic disorders, and aging [16] all of which are linked to abnormally low BAT activity [2,12,39]. Increasing evidence indicates that blockade of circulating ACBP could benefit multiple organs [56]. Although our data suggest that ACBP-mediated repression of BAT activity primarily results from local up-regulation of ACBP expression and release by BAT, it is likely that elevated systemic levels of ACBP also exert repressive effects on BAT activity. Given the strong link between high BAT activity and cardiometabolic health, our findings imply that ACBP's inhibitory effects on BAT may contribute to the ability of elevated ACBP levels to negatively impact systemic metabolic conditions. Moreover, the action of ACBP may be envisioned as a tool to prevent pathogenic conditions associated with BAT hyperactivity, such as cachexia in some types of cancer and hypermetabolism of severe burn patients [57].

## ACKNOWLEDGEMENTS

We thank C. Wolfrum for facilitating access to snRNAseq databases and M. Morales for technical support.

## CRediT AUTHORSHIP CONTRIBUTION STATEMENT

**Albert Blasco-Roset:** Writing — original draft, Investigation, Formal analysis, Data curation, Conceptualization. **Tania Quesada-López:** Investigation, Formal analysis, Data curation. **Alberto Mestres-Arenas:** Methodology, Investigation. **Joan Villarroya:** Investigation, Formal analysis. **Francisco J. Godoy-Nieto:** Formal analysis, Data curation. **Rubén Cereijo:** Formal analysis, Data curation. **Celia Rupérez:** Methodology, Investigation. **Ditte Neess:** Methodology, Investigation. **Nils J. Færgeman:** Writing — review & editing, Investigation. **Marta Giralt:** Writing — review & editing, Investigation. **Anna Planavila:** Writing — review & editing, Conceptualization. **Francesc Villarroya:** Writing — review & editing, Writing — original draft, Funding acquisition, Conceptualization.

## DECLARATION OF COMPETING INTEREST

The authors declare that they have no known competing financial interests or personal relationships that could have appeared to influence the work reported in this paper.

## FUNDING SOURCES

We thank the State Agency of Research (AEI) of the Spanish Ministry of Science (MCIN) for funding. This research was supported by grants PID2020-114112RB-I00, CNS2022-135516 and PID2023-1467810-

 

I00 funded by MICIN/AEI/10.13039/50110 0011033 and FEDER, UE. A.B-R. was supported by a FI-SDUR Ph. D. scholarship (grant 2021 FISDU 00256), and A.M-A by a PhD scholarship (grant FPU20/03364) funded by MICIN/AEI/10.13039/50110 0011033 and FSE+. T.Q-L. is a "Juan de la Cierva-Incorporación" researcher (grant IJC2020-043380-I funded by the MCIN/AEI/10.13039/501100011033 and by the European Union Next Generation EU/PRTR).

## DATA AVAILABILITY

Data will be made available on request.

## APPENDIX A. SUPPLEMENTARY DATA

Supplementary data to this article can be found online at https://doi.org/10.1016/j.molmet.2025.102153.

## REFERENCES

[1] Lowell BB, Susulic VS, Hamann A, Lawitts JA, Himms-Hagen J, Boyer BB, et al. Development of obesity in transgenic mice after genetic ablation of brown adipose tissue. Nature 1993;366:740–2. https://doi.org/10.1038/366740a0.

[2] Becher T, Palanisamy S, Kramer DJ, Eljalby M, Marx SJ, Wibmer AG, et al. Brown adipose tissue is associated with cardiometabolic health. Nat Med 2021;27:58–65. https://doi.org/10.1038/s41591-020-1126-7.

[3] Feldmann HM, Golozoubova V, Cannon B, Nedergaard J. UCP1 ablation induces obesity and abolishes diet-induced thermogenesis in mice exempt from thermal stress by living at thermoneutrality. Cell Metab 2009;9:203–9. https://doi.org/10.1016/j.cmet.2008.12.014.

[4] Cannon B, Nedergaard J. Brown adipose tissue: function and physiological significance. Physiol Rev 2004;84:277–359. https://doi.org/10.1152/physrev.00015.2003.

[5] Giralt M, Villarroya F. Mitochondrial uncoupling and the regulation of glucose homeostasis. Curr Diabetes Rev 2016;13:386–94. https://doi.org/10.2174/1573399812666160217122707.

[6] Bartelt A, Bruns OT, Reimer R, Hohenberg H, Ittrich H, Peldschus K, et al. Brown adipose tissue activity controls triglyceride clearance. Nat Med 2011;17:200–5. https://doi.org/10.1038/nm.2297.

[7] Villarroya F, Cereijo R, Villarroya J, Giralt M. Brown adipose tissue as a secretory organ. Nat Rev Endocrinol 2017;13:26–35. https://doi.org/10.1038/nrendo.2016.136.

[8] Beijer E, Schoenmakers J, Vijgen G, Kessels F, Dingemans A, Schrauwen P, et al. A role of active brown adipose tissue in cancer cachexia? Onco Rev 2012;6:e11. https://doi.org/10.4081/oncol.2012.e11.

[9] Seki T, Yang Y, Sun X, Lim S, Xie S, Guo Z, et al. Brown-fat-mediated tumour suppression by cold-altered global metabolism. Nature 2022;608:421–8. https://doi.org/10.1038/s41586-022-05030-3.

[10] Patsouris D, Qi P, Abdullahi A, Stanojcic M, Chen P, Parousis A, et al. Burn induces browning of the subcutaneous white adipose tissue in mice and humans. Cell Rep 2015;13:1538–44. https://doi.org/10.1016/j.celrep.2015.10.028.

[11] Villarroya F, Vidal-Puig A. Beyond the sympathetic tone: the new brown fat activators. Cell Metab 2013;17:638–43. https://doi.org/10.1016/j.cmet.2013.02.020.

[12] Zoico E, Rubele S, De Caro A, Nori N, Mazzali G, Fantin F, et al. Brown and beige adipose tissue and aging. Front Endocrinol 2019;10:368. https://doi.org/10.3389/fendo.2019.00368.

[13] Alquier T, Christian-Hinman CA, Alfonso J, Færgeman N. From benzodiazepines to fatty acids and beyond: revisiting the role of ACBP/DBI. Trends Endocrinol Metabol 2021;32:890–903. https://doi.org/10.1016/j.tem.2021.08.009.

[14] Neess D, Kruse V, Marcher A, Wæde MR, Vistisen J, Møller PM, et al. Epidermal Acyl-CoA-binding protein is indispensable for systemic energy homeostasis. Mol Metabol 2021;44:101144.

[15] Bravo-San Pedro JM, Sica V, Martins I, Pol J, Loos F, Maiuri MC, et al. Acyl-CoA-Binding protein is a lipogenic factor that triggers food intake and obesity. Cell Metab 2019;30:754–67. https://doi.org/10.1016/j.cmet.2019.07.010.

[16] Montégut L, Abdellatif M, Motiño O, Madeo F, Martins I, Quesada V, et al. Acyl coenzyme A binding protein (ACBP): an aging- and disease-relevant "autophagy checkpoint.". Aging Cell 2023;22:e13910. https://doi.org/10.1111/acel.13910.

[17] Ruperez C, Blasco-Roset A, Kular D, Cairo M, Ferrer-Curriu G, Villarroya J, et al. Autophagy is involved in cardiac remodeling in response to environmental temperature change. Front Physiol 2022;13:864427. https://doi.org/10.3389/fphys.2022.864427.

[18] Quesada-López T, Cereijo R, Turatsinze J, Planavila A, Cairó M, Gavaldà-Navarro A, et al. The lipid sensor GPR120 promotes brown fat activation and FGF21 release from adipocytes. Nat Commun 2016;7:13479. https://doi.org/10.1038/ncomms13479.

[19] Mestres-Arenas A, Cairó M, Peyrou M, Villarroya F. Blood sampling for arteriovenous diference measurements across interscapular brown adipose tissue in rat. Methods Mol Biol 2022;2448:273–82. https://doi.org/10.1007/978-1-0716-2087-8.

[20] Cairó M, Villarroya J, Cereijo R, Campderrós L, Giralt M, Villarroya F. Thermogenic activation represses autophagy in brown adipose tissue. Int J Obes 2016;40:1591–9. https://doi.org/10.1038/ijo.2016.115.

[21] Yeo CR, Agrawal M, Hoon S, Shabbir A, Shrivastava MK, Huang S, et al. SGBS cells as a model of human adipocyte browning: a comprehensive comparative study with primary human white subcutaneous adipocytes. Sci Rep 2017;7:4031. https://doi.org/10.1038/s41598-017-04369-2.

[22] Singh R, Xiang Y, Wang Y, Baikati K, Cuervo AM, Luu YK, et al. Autophagy regulates adipose mass and differentiation in mice. J Clin Investig 2009;119:3329–39. https://doi.org/10.1172/JCI39228.

[23] Li Y, Fromme T, Schweizer S, Schöttl T, Klingenspor M. Taking control over intracellular fatty acid levels is essential for the analysis of thermogenic function in cultured primary brown and brite/beige adipocytes. EMBO Rep 2014;15:1069–76. https://doi.org/10.15252/embr.201438775.

[24] Halurkar MS, Inoue O, Singh A, Mukherjee R, Ginugu M, Ahn C, et al. The widely used Ucp1-Cre transgene elicits complex developmental and metabolic phenotypes. Nat Commun 2025;16:770. https://doi.org/10.1038/s41467-024-54763-4.

[25] Szklarczyk D, Gable AL, Nastou KC, Lyon D, Kirsch R, Pyysalo S, et al. The STRING database in 2021: customizable protein-protein networks, and functional characterization of user-uploaded gene/measurement sets. Nucleic Acids Res 2021;49:D605–12. https://doi.org/10.1093/nar/gkaa1074.

[26] Stuart T, Butler A, Hoffman P, Hafemeister C, Papalexi E, Mauck 3rd WM, et al. Comprehensive integration of single cell data. Cell 2019;177:1888–902. https://doi.org/10.1016/j.cell.2019.05.031.

[27] Becht E, McInnes L, Healy J, Dutertre C, Kwok IWH, Ng LG, et al. Dimensionality reduction for visualizing single-cell data using UMAP. Nat Biotechnol 2018;37:38–44. https://doi.org/10.1038/nbt.4314.

[28] Neess D, Bloksgaard M, Bek S, Marcher A, Elle IC, Helledie T, et al. Disruption of the acyl-CoA-binding protein gene delays hepatic adaptation to metabolic changes at weaning. J Biol Chem 2011;286:3460–72. https://doi.org/10.1074/jbc.M110.161109.

[29] Domingo P, Quesada-López T, Villarroya J, Cairó M, Gutierrez MM, Mateo MG, et al. Differential effects of dolutegravir, bictegravir and raltegravir in adipokines and inflammation markers on human adipocytes. Life Sci 2022;308:120948. https://doi.org/10.1016/j.lfs.2022.120948.

[30] Fromme T, Klingenspor M. Uncoupling protein 1 expression and high-fat diets. Am J Physiol Regul Integr Comp Physiol 2011;300:R1–8. https://doi.org/10.1152/ajpregu.00411.2010.

 

[31] Sun W, Dong H, Balaz M, Slyper M, Drokhlyansky E, Colleluori G, et al. snRNA-seq reveals a subpopulation of adipocytes that regulates thermogenesis. Nature 2020;587:98—102. https://doi.org/10.1038/s41586-020-2856-x.

[32] Collins S. beta-Adrenergic receptors and adipose tissue metabolism: evolution of an old story. Annu Rev Physiol 2022;84:1—16. https://doi.org/10.1146/annurev-physiol-060721-092939.

[33] Campderrós L, Moure R, Cairó M, Gavaldà-Navarro A, Quesada-López T, Cereijo R, et al. Brown adipocytes secrete GDF15 in response to thermogenic activation. Obesity 2019;27:1606—16. https://doi.org/10.1002/oby.22584.

[34] Colitti M, Ali U, Wabitsch M, Tews D. Transcriptomic analysis of Simpson Golabi Behmel syndrome cells during differentiation exhibit BAT-like function. Tissue Cell 2022;77:101822. https://doi.org/10.1016/j.tice.2022.101822.

[35] Duran JM, Anjard C, Stefan C, Loomis WF, Malhotra V. Unconventional secretion of Acb1 is mediated by autophagosomes. J Cell Biol 2010;188:527—36. https://doi.org/10.1083/jcb.200911154.

[36] Bjørkøy G, Lamark T, Pankiv S, Øvervatn A, Brech A, Johansen T, et al. Monitoring autophagic degradation of p62/SQSTM1. Methods Enzymol 2009;452:181—97. https://doi.org/10.1016/S0076-6879(08)03612-4.

[37] Nedergaard J, Cannon B. UCP1 mRNA does not produce heat. Biochim Biophys Acta 2013;1831:943—9.

[38] Kang S, Bajnok L, Longo KA, Petersen RK, Hansen JB, Kristiansen K, et al. Effects of Wnt signaling on brown adipocyte differentiation and metabolism mediated by PGC-1α. Mol Cell Biol 2005;25:1272—82. https://doi.org/10.1128/mcb.25.4.1272-1282.2005.

[39] Villarroya F, Cereijo R, Villarroya J, Gavaldà-Navarro A, Giralt M. Toward an understanding of how immune cells control brown and beige adipobiology. Cell Metab 2018;27:954—61. https://doi.org/10.1016/j.cmet.2018.04.006.

[40] Puigserver P, Wu Z, Park CW, Graves R, Wright M, Spiegelman BM, et al. A cold-inducible coactivator of nuclear receptors linked to adaptive thermogenesis. Cell 1998;92:829—39. https://doi.org/10.1016/S0092-8674(00)81410-5.

[41] Bianco AC, McAninch EA. The role of thyroid hormone and brown adipose tissue in energy homoeostasis. Lancet Diabetes Endocrinol 2013;1:250—8. https://doi.org/10.1016/S2213-8587(13)70069-X.

[42] Kumar N, Liu D, Wang H, Robidoux J, Collins S. Orphan nuclear receptor NOR-1 enhances 3′,5′-cyclic adenosine 5′-monophosphate-dependent uncoupling protein-1 gene transcription. Mol Endocrinol 2008;22:1057—64. https://doi.org/10.1210/me.2007-0464.

[43] Onder Y, Laothamatas I, Berto S, Sewart K, Kilaru G, Bordieanu B, et al. The circadian protein nocturnin regulates metabolic adaptation in brown adipose tissue. iScience 2019;19:83—92. https://doi.org/10.1016/j.isci.2019.07.016.

[44] Wang G, Zhao X, Meng Z, Kern M, Dietrich A, Chen Z, et al. The brown fat-enriched secreted factor Nrg4 preserves metabolic homeostasis through attenuation of hepatic lipogenesis. Nat Med 2014;20:1436—43. https://doi.org/10.1038/nm.3713.

[45] Reddy JK, Goel SK, Nemali MR. Transcriptional regulation of peroxisomal fatty acyl-CoA oxidase and enoyl-CoA hydratase/3-hydroxyacyl-CoA dehydrogenase in rat liver by peroxisome proliferators. Proc Natl Acad Sci U S A 1986;83:1747—51. https://doi.org/10.1073/pnas.83.6.1747.

[46] Barbera MJ, Schluter A, Pedraza N, Iglesias R, Villarroya F, Giralt M. Peroxisome proliferator-activated receptor α activates transcription of the brown fat uncoupling protein-1 gene. A link between regulation of the thermogenic and lipid oxidation pathways in the brown fat cell. J Biol Chem 2001;276:1486—93. https://doi.org/10.1074/jbc.M006246200.

[47] Cereijo R, Gavaldà-Navarro A, Cairó M, Quesada-López T, Villarroya J, Morón-Ros S, et al. CXCL14, a brown adipokine that mediates brown-fat-to-macrophage communication in thermogenic adaptation. Cell Metab 2018;28:750—63. https://doi.org/10.1016/j.cmet.2018.07.015.

[48] Cao W, Daniel KW, Robidoux J, Puigserver P, Medvedev AV, Bai X, et al. p38 mitogen-activated protein kinase is the central regulator of cyclic AMP-dependent transcription of the brown fat uncoupling protein 1 gene. Mol Cell Biol 2004;24:3057—67. https://doi.org/10.1128/mcb.24.7.3057-3067.2004.

[49] Villarroya F, Peyrou M, Giralt M. Transcriptional regulation of the uncoupling protein-1 gene. Biochim 2017;134:86—92. https://doi.org/10.1016/j.biochi.2016.09.017.

[50] Sustarsic EG, Ma T, Lynes MD, Larsen M, Karavaeva I, Havelund JF-, et al. Cardiolipin synthesis in brown and beige fat mitochondria is essential for systemic energy homeostasis. Cell Metab 2018;28:159—74. https://doi.org/10.1016/j.cmet.2018.05.003.

[51] Joseph A, Chen H, Anagnostopoulos G, Montégut L, Lafarge A, Motiño O, et al. Effects of acyl-coenzyme A binding protein (ACBP)/diazepam-binding inhibitor (DBI) on body mass index. Cell Death Dis 2021;12:599. https://doi.org/10.1038/s41419-021-03864-9.

[52] Anagnostopoulos G, Motiño O, Li S, Carbonnier V, Chen H, Sica V, et al. An obesogenic feedforward loop involving PPARγ, acyl-CoA binding protein and GABAA receptor. Cell Death Dis 2022;13:356. https://doi.org/10.1038/s41419-022-04834-5.

[53] Sica V, Martins I, Motiño O, Bravo-San Pedro JM, Kroemer G. Antibody-mediated neutralization of ACBP/DBI has anorexigenic and lipolytic effects. Adipocyte 2020;9:116—9. https://doi.org/10.1080/21623945.2020.1736734.

[54] Peyrou M, Cereijo R, Quesada-López T, Campderrós L, Gavaldà-Navarro A, Liñares-Pose L, et al. The kallikrein—kinin pathway as a mechanism for auto-control of brown adipose tissue activity. Nat Commun 2020;11:2132. https://doi.org/10.1038/s41467-020-16009-x.

[55] Whittle AJ, Jiang M, Peirce V, Relat J, Virtue S, Ebinuma H, et al. Soluble LR11/SorLA represses thermogenesis in adipose tissue and correlates with BMI in humans. Nat Commun 2015;6:8951. https://doi.org/10.1038/ncomms9951.

[56] Motiño O, Lambertucci F, Anagnostopoulos G, Li S, Nah J, Castoldi F, et al. ACBP/DBI protein neutralization confers autophagy-dependent organ protection through inhibition of cell loss, inflammation, and fibrosis. Proc Natl Acad Sci USA 2022;119:e2207344119. https://doi.org/10.1073/pnas.2207344119.

[57] Huang L, Zhu L, Zhao Z, Jiang S. Hyperactive browning and hypermetabolism: potentially dangerous element in critical illness. Front Endocrinol 2024;15:1484524. https://doi.org/10.3389/fendo.2024.1484524.

 